I&EC research
Industrial & Engineering Chemistry Research

Article

pubs.acs.org/IECR

Improved Model Formulations for Multiperiod Hydrogen Network Designs

Che-Chi Kuo and Chuei-Tin Chang*

Department of Chemical Engineering, National Cheng Kung University, Tainan, Taiwan 70101

Supporting Information

ABSTRACT: Operating cost reduction and/or air pollution abatement via hydrogen integration is a research issue that has recently attracted considerable attention in the petroleum refining industries. Although a number of mathematical programming models have been developed to generate the optimal hydrogen distribution schemes, there is still room for further improvement. In particular, the primary deficiencies in current modeling practices can be attributed to (1) unreasonable unit models of the hydrogen users and producers and (2) incomprehensive design considerations. The conventional models of hydrogen users (such as the hydrotreater and hydrocracker) were usually formulated according to fixed throughputs and also constant feed and product concentrations. On the basis of the shortcut calculation method proposed in this study, not only these inlet and outlet flow rates and concentrations can be treated as decision variables but also their interactions can be characterized with more consistent material-balance constraints. On the other hand, because every hydrogen producer, e.g., the steam reforming plant, was regarded only as a simple hydrogen source in the past, the more rigorous models of its embedded units are built and incorporated in the improved mathematical program. As a result of these modifications, better design options can be identified in the present study. To ensure comprehensive design considerations, all often-encountered seasonal variations in model parameters and options to add extra compressors, purifiers, and fuel cells are considered in a novel multiperiod formulation. Furthermore, as an alternative to numerically solving this model, a systematic timesharing algorithm is also devised to manually integrate the conventional single-period designs to form a less economical but more flexible network structure for operations in all periods. Finally, extensive case studies have been carried out to test the proposed design methods, and three examples are reported.

1. INTRODUCTION

The growing demand for hydrogen in the modern petroleum industry can be attributed to the needs for producing better products and also for satisfying more stringent environmental regulations. There may be several different hydrogen users in a refinery. The raw material (petroleum) can be converted to various transportation fuels and petrochemical feedstocks in the hydrocracking processes, while the sulfur contents in these products can be reduced with the hydrotreating units. As a result of the increasingly high consumption level, the development of an efficient scheme for hydrogen integration and distribution within a given oil refining process has become a popular research issue in recent years.

Two alternative design strategies, i.e., the pinch (or graphic) method and the mathematical programming method, have traditionally been adopted for optimal resource integration in chemical plants. Generally speaking, the same approaches were also followed in the published studies to synthesize the hydrogen networks. The related literature is summarized as follows:

Towler et al.[1] and Alves and Towler[2] first developed a novel pinch method for hydrogen integration in their pioneering works. Without imposing pressure constraints on the source-sink matches, the minimum hydrogen consumption rate of a given system was determined on the basis of a residue curve similar to that utilized in HEN design. El-Halwagi et al.[3] later suggested to calculate the target usage level of a particular resource with the corresponding composite curves. This general approach is certainly also applicable in the special case of hydrogen network design. Zhao et al.[4] then applied the pinch strategy to synthesize a multicomponent hydrogen network, while Ding et al.[5] further considered pressure bounds in practical applications. Zhang et al.[6] introduced a "triangle rule" to incorporate the design options of hydrogen recovery and recycle into the composite curves. Finally, Zhang et al.[7] made use of the graphic method to identify the minimum resource demand in a multicomponent system. It can be observed from the above publications that, although the graphical approach can be adopted to acquire intuitive insight for locating bottleneck(s) so as to improve resource utilization, it is still ineffective for quantitative evaluation of the relatively large and complex hydrogen networks in realistic refineries.

To perform the design calculations more rigorously and efficiently, a number of mathematical programming models have been developed in recent years. Hallale and Liu[8] proposed a superstructure-based modeling procedure that incorporates pressure considerations. The optimal capacities of new units to be purchased and the best network configuration can be simultaneously identified with such a model. Van den Heever and Grossmann[9] formulated a mathematical program for solving the planning and scheduling problems of hydrogen

Received: September 23, 2014
Revised: November 22, 2014
Accepted: December 5, 2014
Published: December 5, 2014

dx.doi.org/10.1021/ie5037726 | Ind. Eng. Chem. Res. 2014, 53, 20204−20222

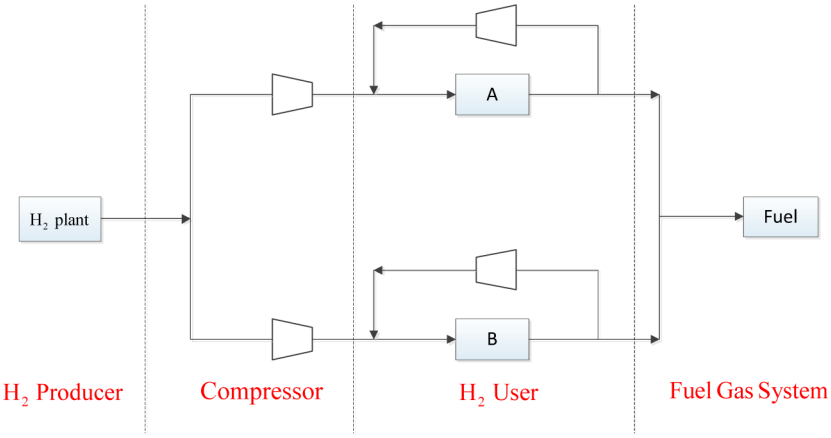

Figure 1. Traditional hydrogen network structure.

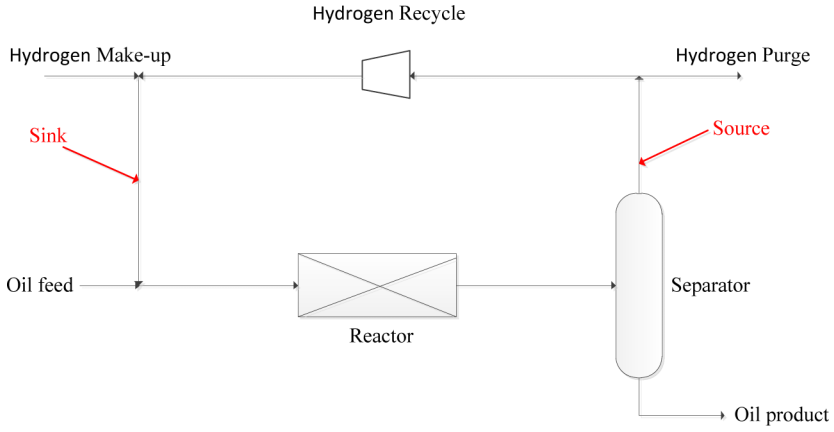

Figure 2. Common process structure of hydrogen users.

supply chains. Liu and Zhang[10] introduced the pressure swing adsorption (PSA) unit(s) into the network design so as to improve hydrogen utilization efficiency. Khajehpour et al.[11] suggested to simplify the superstructure with heuristic rules for the purpose of enhancing solution reliability. Kumar et al.[12] and Liao et al.[13] both modified and improved the conventional models from new perspectives. Jia and Zhang[14] tried to optimize the multicomponent hydrogen systems, while Zhou et al.[15] integrated one with a mass exchanger network (MEN) for H_2S removal. To further reduce the overall hydrogen consumption rate, Jiao et al.[16] implemented additional model changes by treating the total flow rate and component concentrations at the inlet of every hydrogen user as decision variables. For the purpose of promoting solution efficiency, they also developed a two-step optimization strategy by replacing the original mixed-integer nonlinear program (MINLP) with MILPs. Wu et al.[17] followed essentially the same modeling practice but also imposed inequality constraints at the inlets of hydrogen users. In a subsequent study, Wu et al.[18] developed two mathematical programming models to determine separately the minimum energy consumption rate and minimum number of compressors in a hydrogen distribution system. Finally, Chiang and Chang[19] proposed to use a multiobjective design approach to address both economic and environmental issues for hydrogen networks that incorporate fuel cells.

Despite previous developments of various mathematical programming models for generating the optimal hydrogen integration and distribution schemes, there is still room for further improvements. Generally speaking, the applicability of available formulations is severely hampered by two common deficiencies, i.e., (1) oversimplified unit models and (2) incomprehensive design considerations:

(1) The hydrotreaters and hydrocrackers were unreasonably described in the past according to fixed operating conditions and, also, the steam reforming plant was modeled simply as a hydrogen provider without any provisions for possible recycle. Although Jiao et al.[16] and Wu et al.[17] allowed the inlet flow rates and concentrations of hydrogen users to vary, their models were still logically inconsistent because the corresponding outlet conditions were treated as constants.

(2) The often-encountered seasonal variations in model parameters and the design options to add extra compressors, purifiers, and fuel cells were often ignored in the conventional approach. Although Ahmad et al.[20] proposed a programming model to generate flexible network configurations which are suitable for operation in multiple periods, this approach is limited to cases in which only the throughputs of hydrogen users were time-dependent.

Thus, this study aims to circumvent the above drawbacks by modifying the conventional models. In particular, there are three specific tasks to be accomplished: (1) to improve the unit model of hydrogen users, (2) to model the steam reformer and add it into the overall mathematical program, and (3) to develop the multiperiod hydrogen network design methods.

dx.doi.org/10.1021/ie5037726 | *Ind. Eng. Chem. Res.* 2014, 53, 20204−20222

The remainder of this paper is organized as follows. The updated version of a superstructure is first described in the next section. The improved models of the hydrogen users, the fuel gas system, and all units in the hydrogen production plant are then presented in the third section. For comparison convenience, all conventional unit models are also given in the Appendix. Section 4 outlines the MINLP model for single-period hydrogen network designs together with an illustrative example. Two effective multiperiod design strategies are then described in section 5, and a second example is also provided to show the benefits of the proposed design strategies. The feasibility and usefulness of these strategies are further demonstrated with additional case studies in the sixth section. Finally, conclusions are presented in section 7.

2. SUPERSTRUCTURE

It is assumed in this work that the typical structure of existing hydrogen networks can be represented with the sketch given in Figure 1. The hydrogen producer(s), compressors, hydrogen users, and fuel gas system are arranged sequentially in distinct steps, while multiple units of the same type may be placed in parallel. The goal of the present study can be considered as optimally restructuring this given network with the available units and also new ones when necessary.

The mathematical programming model in this work is formulated on the basis of a superstructure, which is essentially a collection of all possible links between hydrogen sources and sinks. For illustration convenience, let us first consider the common structure of hydrogen users (see Figure 2). In this process, the reactor inlet can be associated with a sink in superstructure and the overhead exit of separator a source. On the basis of the same principle, the suction and discharge ends of a compressor can be viewed as sink and source, respectively. The fuel gas system is obviously a sink only, while the hydrogen plant is usually treated as a simple source in the conventional programming models. If the new units are excluded from consideration, the following three connection rules can be applied directly for building the superstructure:

i. A feasible source-sink link can be established if the corresponding pressure drop is non-negative and also the concentration lower bound at the sink is achievable.
ii. If the sink of a connection is associated with the suction side of a compressor, then its discharge pressure should not be lower than that of the source.
iii. Any self-recycle stream around a compressor is not allowed.

The possible new units considered in this work include fuel cells, compressors, and pressure swing adsorption (PSA) units, and each can serve both as a source and a sink. If it is desired to evaluate the benefits of adding these units, their operating pressures must also be properly selected. Because there may be more than one choice, an exhaustive list of all alternative source and sink pressures for every such unit should be produced according to the systematic procedure described in Chiang and Chang,[19] and the additional feasible links caused by these new units can then be identified with the aforementioned connection rules. For the sake of brevity, the superstructure construction steps are not repeated here.

To facilitate model formulation, let us first assign a distinct label to each unit embedded in the superstructure and then classify and collect these labels in the following two sets to identify their sources and sinks, respectively:

$\mathbf{I} = \{i \mid i \text{ denotes the label of a hydrogen source in superstructure}\}$

$\mathbf{J} = \{j \mid j \text{ denotes the label of a hydrogen sink in superstructure}\}$

It is important to note that, because the label of every unit is used to identify both its source and its sink, some elements of **I** and **J** are identical.

As mentioned before, it may be beneficial to introduce a few new units, i.e., the additional compressors, PSA units, and fuel cells, into a hydrogen network design. To facilitate concise formulation, let us define the following label sets:

$\mathbf{NEQ} = \{\text{neq} \mid \text{neq is the label of a new unit which is not present in the existing network}\}$

$\mathbf{COM}' = \{\text{com} \mid \text{com is the label of a new compressor which is not present in the existing network}\}$

$\mathbf{COM} = \{\text{com} \mid \text{com is the label of a compressor embedded in the superstructure}\}$

$\mathbf{PUR}' = \{\text{pur} \mid \text{pur is the label of a new purifier which is not present in the existing network}\}$

$\mathbf{PUR} = \{\text{pur} \mid \text{pur is the label of a purifier embedded in the superstructure}\}$

$\mathbf{FC}' = \{\text{fc} \mid \text{fc is the label of a new fuel cell which is not present in the existing network}\}$

$\mathbf{FC} = \{\text{fc} \mid \text{fc is the label of a fuel cell embedded in the superstructure}\}$

Therefore, $\mathbf{NEQ} = \mathbf{COM}' \cup \mathbf{PUR}' \cup \mathbf{FC}'$, $\mathbf{COM}' \subset \mathbf{COM}$, $\mathbf{PUR}' \subset \mathbf{PUR}$, $\mathbf{FC}' \subset \mathbf{FC}$, and the corresponding logic constraints in the mathematical programming model can be formulated as

$$e_{\text{neq}} B^{\text{L}}_{\text{neq}} \le \sum_{i \in \mathbf{I}} F_{i,\text{neq}} \le e_{\text{neq}} B^{\text{U}}_{\text{neq}} \tag{1}$$

$$\sum_{\text{com} \in \mathbf{COM}'} e_{\text{com}} \le N_{\text{comp}} \tag{2}$$

$$\sum_{\text{pur} \in \mathbf{PUR}'} e_{\text{pur}} \le N_{\text{PSA}} \tag{3}$$

$$\sum_{\text{fc} \in \mathbf{FC}'} e_{\text{fc}} \le N_{\text{fcell}} \tag{4}$$

where $\text{neq} \in \mathbf{NEQ}$; $F_{i,\text{neq}}$ denotes the flow rate of a stream in superstructure between source i and the sink end of unit neq; $e_{\text{neq}} \in \{0,1\}$ is a binary variable denoting if unit neq is adopted in the network design; $B^{\text{L}}_{\text{neq}}$ and $B^{\text{U}}_{\text{neq}}$ denote the lower and upper capacity limits of unit neq, respectively; $e_{\text{com}} \in \{0,1\}$ is a binary variable denoting if compressor com is chosen, and N_{comp} is the maximum number of new compressors allowed in design; $e_{\text{pur}} \in \{0,1\}$ is a binary variable denoting if purifier pur is chosen, and N_{PSA} is the maximum number of new PSA units allowed in the design; $e_{\text{fc}} \in \{0,1\}$ is a binary variable denoting if

dx.doi.org/10.1021/ie5037726 | Ind. Eng. Chem. Res. 2014, 53, 20204−20222

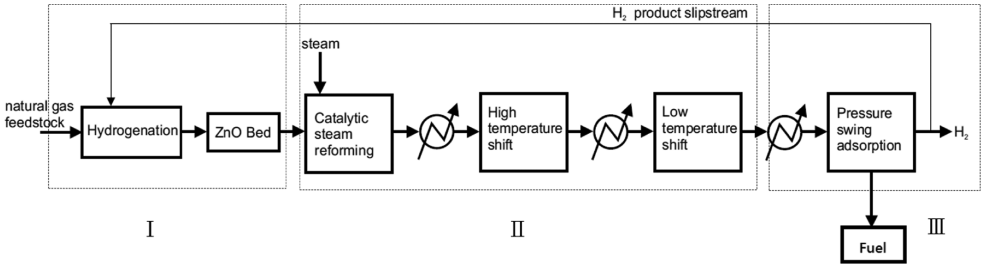

Figure 3. General structure of steam reforming process.

fuel cell fc is chosen, and N_{fcell} is the maximum number of new fuel cells allowed in design.

Because of the presence of the aforementioned new units, it is necessary to distinguish the corresponding connections in a superstructure

$$\mathbf{PIPE} = \{(i,j) \mid (i,j) \text{ is the connection between source } i \text{ and sink } j \text{ in the superstructure}\}$$

$$\mathbf{PIPE}_{\text{o}} = \{(i,j) \mid (i,j) \text{ is the connection between source } i \text{ and sink } j \text{ in the existing network}\}$$

$$\mathbf{PIPE}' = \mathbf{PIPE}/\mathbf{PIPE}_{\text{o}}$$

Because usually not every new connection is chosen in the final design, the following logic constraints must also be imposed

$$e_{i,j}^{\text{pipe}} B_{i,j}^{\text{L}} \le F_{i,j} \le e_{i,j}^{\text{pipe}} B_{i,j}^{\text{U}} \tag{5}$$

where $(i,j) \in \mathbf{PIPE}'$; $F_{i,j}$ denotes the flow rate of the stream between source i and sink j; $e_{i,j}^{\text{pipe}} \in \{0,1\}$ is a binary variable denoting if connection (i,j) is adopted in the network design; $B_{i,j}^{\text{L}}$ and $B_{i,j}^{\text{U}}$ denote the lower and upper flow rate limits of the stream, respectively, between source i and sink j.

3. IMPROVED UNIT MODELS

For the sake of completeness, the conventional model formulations of all units in superstructure are provided in the Appendix. Only the unit models of the hydrogen users, the steam reforming plant, and the fuel gas system have been modified in the present work. Notice that, other than hydrogen, methane is usually the most abundant component in almost every stream in the hydrogen network. Thus, for the sake of computation simplicity, the species methane is assumed to be the sole impurity in every hydrogen-containing stream,[8] and the natural gas supply is treated as a source with 0 vol % hydrogen. On the basis of this assumption, the improved unit models can be formulated and outlined as described in the following.

3.1. Hydrogen Users. From eqs A.1−A.4 in the Appendix, it can be observed that the inlet and outlet conditions are fixed in the conventional models. Because this practice clearly precludes other feasible options which may also be favorable, these constants are replaced with variables in the improved model to facilitate more complete consideration. In addition, the hydrogen consumption rate of each unit is assumed to be kept at an a priori given value ($\overline{f}_{\text{sk}}^{\text{H}_2}$) in the present study based on the argument that the production rates of fuels and petrochemicals in a refinery are usually targeted in advance. Note that such an assumption implies that the overall generation rate of all other gases can also be treated as an unchanged parameter ($\overline{f}_{\text{sr}}^{\text{CH}_4}$). Therefore, the model constraints at the sink end of a hydrogen user can be written as

$$\sum_{i \in \mathbf{I}} F_{i,\text{sk}} = f_{\text{sk}} \tag{6}$$

$$\sum_{i \in \mathbf{I}} F_{i,\text{sk}} y_i = f_{\text{sk}} y_{\text{sk}} \tag{7}$$

$$f_{\text{sk}} y_{\text{sk}} \ge \overline{fy}_{\text{sk}}^{\min} \tag{8}$$

$$y_{\text{sk}} \ge \overline{y}_{\text{sk}}^{\min} \tag{9}$$

where sk ∈ **SK** and **SK** is a label set for identifying the inlets of hydrogen using units; f_{sk} and y_{sk} are variables denoting the total flow rate and hydrogen concentration at inlet sk, respectively; $F_{i,\text{sk}}$ is also a variable which denotes the flow rate of the gas stream from source i to sink sk; $\overline{fy}_{\text{sk}}^{\min}$ and $\overline{y}_{\text{sk}}^{\min}$ are design parameters representing the lower bounds of the inlet hydrogen flow rate and concentration, respectively. On the other hand, the model constraints at the source end can be expressed as

$$\sum_{j \in \mathbf{J}} F_{\text{sr},j} = f_{\text{sr}} \tag{10}$$

$$f_{\text{sr}} = f_{\text{sk}} - \overline{f}_{\text{sr}}^{\text{H}_2} + \overline{f}_{\text{sr}}^{\text{CH}_4} \quad \forall\ \text{sr} = \text{sk} \tag{11}$$

$$f_{\text{sr}} y_{\text{sr}} = f_{\text{sk}} y_{\text{sk}} - \overline{f}_{\text{sr}}^{\text{H}_2} \quad \forall\ \text{sr} = \text{sk} \tag{12}$$

$$y_{\text{sr}} \le \overline{y}_{\text{sr}}^{\max} \tag{13}$$

where, $sr \in \mathbf{SR}$ and **SR** is a label set for identifying the outlets of hydrogen users; f_{sr} and y_{sr} are variables denoting the total flow rate and hydrogen concentration, respectively, at outlet sr; $F_{\text{sr},j}$ is a variable which denotes the flow rate of the gas stream from source sr to sink j; $\overline{f}_{\text{sr}}^{\text{H}_2}$ and $\overline{f}_{\text{sr}}^{\text{CH}_4}$ are a priori given model parameters which are used to represent the hydrogen consumption rate and the net rate of generation of all other gases, respectively; $\overline{y}_{\text{sr}}^{\max}$ denotes the upper bound of hydrogen concentration at source sr, which is imposed primarily to reflect the practical limit of separator within the hydrogen-using process.

3.2. Hydrogen Production Plant. Figure 3 shows the general structure of a typical steam reforming (SR) process.[21] After sulfur is removed via hydrogenation reaction, the feedstock (i.e., natural gas) is then reacted with steam in the catalytic reforming process. The resulting products subsequently go through high- and low-temperature shifts and also the PSA operation in sequence. The purified hydrogen from the PSA unit is consumed in the downstream hydrogen-using processes and also partially recycled to facilitate hydrogenation, while the residue stream of PSA is utilized mainly as fuel.

dx.doi.org/10.1021/ie5037726 | Ind. Eng. Chem. Res. 2014, 53, 20204−20222

As mentioned before, the conventional modeling approach is always to treat the steam reforming plant as a simple source of the hydrogen network without considering interactions between the two. However, because the hydrogen consumption level may be reduced significantly by restructuring the given network, it is clearly desirable to develop schemes that can make good use of the consequent overcapacities in the existing units of the SR process. For this reason, these units are divided into three steps (see steps I, II, and II in Figure 3) and modeled accordingly as described in the following.

3.2.1. Hydrogenation Reaction. Originally, the hydrogen unit in a steam reforming process is used to convert the impurities in feedstock (i.e., methane) to inert components so as to avoid adverse effects on the downstream reactions. Separating the residue hydrogen from its product stream is not always needed unless a relatively large amount of excess hydrogen is fed to ensure maximum conversion. For the purpose of facilitating comprehensive process integration, this unit is viewed in the present study as a regular hydrogen user with the general structure shown in Figure 2. The inlet flow rate of natural gas stream is constrained as follows:

$$F_{\mathrm{NG,H2P_I}} = kZ \tag{14}$$

$$F_{\mathrm{NG,H2P_I}} \le \overline{f}^{\mathrm{NG}}_{\mathrm{H2P_I}} \tag{15}$$

where Z is the generation rate of hydrogen produced with steps I and II, $F_{\mathrm{NG,H2P_I}}$ the feed rate of natural gas, k a proportionality constant that relates $F_{\mathrm{NG,H2P_I}}$ and Z, and $\overline{f}^{\mathrm{NG}}_{\mathrm{H2P_I}}$ the upper bound of natural gas flow rate at the inlet.

On the other hand, the flow rate of the other raw material, i.e., hydrogen, at the inlet of the hydrogenation unit is assumed to be directly proportional to the feed rate of natural gas, i.e.

$$\sum_{i\in\mathbf{I}} F_{i,\mathrm{H2P_I}} y_i = \overline{r}^{\mathrm{in}}_{\mathrm{H/N}} F_{\mathrm{NG,H2P_I}} \tag{16}$$

where $\overline{r}^{\mathrm{in}}_{\mathrm{H/N}}$ is the corresponding coefficient of proportionality. It can be observed from this equation that the hydrogen feedstock may be originated from any source in the hydrogen network. To simplify design calculations, the hydrogen concentration at the inlet is fixed at a given value $\overline{y}^{\mathrm{in}}_{\mathrm{H2P_I}}$:

$$\sum_{i\in\mathbf{I}} F_{i,\mathrm{H2P_I}} y_i = \overline{y}^{\mathrm{in}}_{\mathrm{H2P_I}} \sum_{i\in\mathbf{I}} F_{i,\mathrm{H2P_I}} \tag{17}$$

Finally, the flow rate and concentration of the spent hydrogen stream are also *fixed* at given values in this work according to the conventional model, i.e., eqs A.3 and A.4 in the Appendix. If it is desirable to utilize this stream as a source of the hydrogen network, then positive values should be assigned to both parameters. Otherwise, the flow rate of spent hydrogen stream can be set to zero. This simple-minded modeling approach is primarily due to a lack of published data for establishing more rigorous constraints.

3.2.2. Steam Reforming Reactions.[21,22] The second group of units represents a complex intermediate step that converts natural gas to hydrogen. To simplify computation, linear functions are adopted to characterize the relationships between important variables, i.e.

$$F_{\mathrm{H2P_{II},H2P_{III}}} = \overline{r}_{\mathrm{III/II}} F_{\mathrm{H2P_I,H2P_{II}}} \tag{18}$$

$$\overline{y}^{\mathrm{prod}}_{\mathrm{H2P_{III}}} Z = R_{\mathrm{H2P_{III}}} \overline{y}^{\mathrm{out}}_{\mathrm{H2P_{II}}} F_{\mathrm{H2P_{II},H2P_{III}}} \tag{19}$$

where $F_{\mathrm{H2P_I,H2P_{II}}}$ and $F_{\mathrm{H2P_{II},H2P_{III}}}$ denote the input and output flow rates of step II, respectively, and $\overline{r}_{\mathrm{III/II}}$ is the corresponding proportionality constant; $\overline{y}^{\mathrm{out}}_{\mathrm{H2P_{II}}}$ and $\overline{y}^{\mathrm{prod}}_{\mathrm{H2P_{III}}}$ denote the *known* hydrogen concentrations at the outlets of step II and III, respectively, and $\mathrm{R_{H2P_{III}}}$ is the *constant* hydrogen recovery ratio of the PSA unit in the steam reforming plant. On the basis of the same modeling rationale, all utility consumption rates are also assumed to be directly proportional to the hydrogen generation rate via steps I and II:

$$\mathrm{Stm_{H2P}} = \mathrm{k}'Z \tag{20}$$

$$\mathrm{Pwr_{H2P}} = k''Z \tag{21}$$

$$Q_{\mathrm{H2P}} = \mathrm{k}'''Z \tag{22}$$

where $\mathrm{Stm_{H2P}}$, $\mathrm{Pwr_{H2P}}$, and Q_{H2P} denote the consumption rates of steam, electricity, and heating utility, respectively; k', k'', and k''' represent the corresponding proportionality coefficients.

3.2.3. Pressure Swing Adsorption. Because the PSA unit in the steam reforming plant can be described with the conventional unit model, i.e., eqs A.12−A.18 in the Appendix, the same formulations are not repeated here for the sake of brevity.

3.3. Fuel Gas System. The hydrogen concentration in the product stream of step II is generally believed to be around 75 vol %, i.e., $\overline{y}^{\mathrm{out}}_{\mathrm{H2P_{II}}} \approx 0.75$, while the remaining 25 vol % consists mainly of carbon dioxide (64.9 vol %), methane (18.9 vol %), and carbon monoxide (16.2 vol %). Because a significant percentage of carbon dioxide is present in the residue stream from the PSA unit of the steam reforming plant, the heat generated by the fuel gas system (Q'_{fuel}) may have to be determined with a modified version of the conventional model

$$Q'_{\mathrm{fuel}} = Q_{\mathrm{fuel}} - \Delta H^{\circ}_{\mathrm{c,CH_4}} \frac{\rho^{\circ}_{\mathrm{CH_4}}}{\mathrm{M_{CH_4}}} F_{\mathrm{H2P_{II},H2P_{III}}} (1 - \overline{y}^{\mathrm{out}}_{\mathrm{H2P_{II}}}) \overline{y}^{\mathrm{imp,CO_2}}_{\mathrm{H2P_{II}}} \tag{23}$$

where Q_{fuel} is the heat generation rate determined with eq A.26 in the Appendix; $\rho^{\circ}_{\mathrm{CH_4}}$ is the density of methane under standard conditions, i.e., 0.024 lbm/scf; $\mathrm{M_{CH_4}}$ denotes the molecular weight of methane, i.e., 16.04 g/mol; $\Delta H^{\circ}_{\mathrm{c,CH_4}}$ (=760.88 BTU/mol) denotes the heat of combustion of methane; $\overline{y}^{\mathrm{imp,CO_2}}_{\mathrm{H2P_{II}}} = 0.649$ is the proportion of carbon dioxide in the impurities of the product stream from step II in the steam reforming process.

4. MINLP MODEL FOR SINGLE-PERIOD DESIGNS

The conventional unit models of compressors, PSA units and fuel cells (see sections A.2−A.4 in the Appendix) and the improved formulations presented above can be integrated into a mixed-integer nonlinear program as constraints to produce the optimal single-period design. The objective function used in this optimization problem is the total annual cost (TAC) for restructuring a given hydrogen network, which can be expressed as described in the following.

4.1. Objective Function. The TAC can usually be attributed to the operating and capital costs, i.e.

$$\mathrm{TAC} = \text{Total Annual Operating Cost} + \phi \times \text{Total Capital Cost} \tag{24}$$

dx.doi.org/10.1021/ie5037726 | Ind. Eng. Chem. Res. 2014, 53, 20204−20222

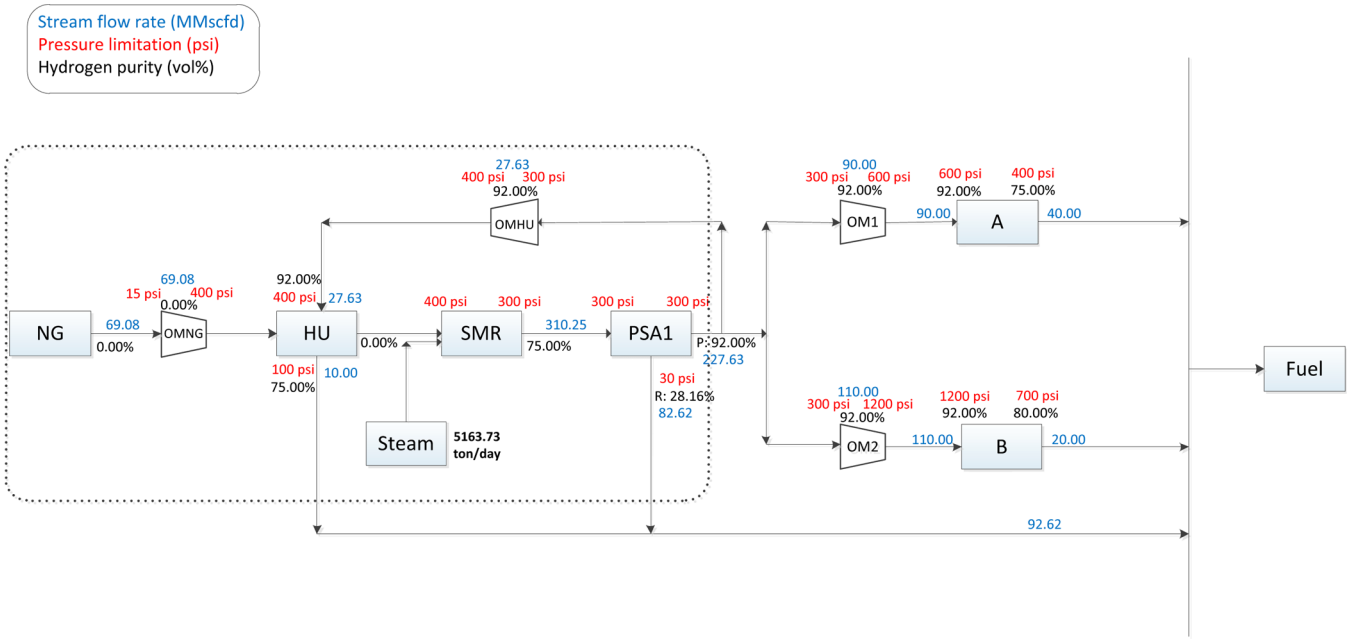

Figure 4. Original hydrogen network in example 1.

The total operating cost in the present application arises from five contributing factors, i.e., the consumption rates of natural gas and steam, the net generation rates of heat and electrical power, and operation and maintenance of fuel cells. Specifically, it is computed according to the following formulas:

$$\text{Total Annual Operating Cost} = \text{Cost}_{\text{NG}} + \text{Cost}_{\text{steam}} - \text{Rvn}_{\text{exfuel}} - \text{Rvn}_{\text{ele}} + \text{Cost}_{\text{OM-fc}} \tag{25}$$

$$\text{Cost}_{\text{NG}} = \text{PI}_{\text{NG}}\bar{H}\sum_{j\in\mathbf{J}} F_{\text{NG,j}} \tag{26}$$

$$\text{Cost}_{\text{steam}} = \text{PI}_{\text{steam}}\bar{H}\text{Stm}_{\text{H2P}} \tag{27}$$

$$\text{Rvn}_{\text{exfuel}} = PI_{\text{fuel}}\bar{H}(Q'_{\text{fuel}} - Q_{\text{H2P}}) \tag{28}$$

$$\text{Rvn}_{\text{ele}} = \text{PI}_{\text{ele}}\bar{H}\Big(\sum_{\text{fc}\in\mathbf{FC}} \text{Pwr}_{\text{fc}} - \sum_{\text{com}\in\mathbf{COM}} \text{Pwr}_{\text{com}} - \text{Pwr}_{\text{H2P}}\Big) \tag{29}$$

$$\text{Cost}_{\text{OM-fc}} = \text{PI}_{\text{fc}}\bar{H}\sum_{\text{fc}\in\mathbf{FC}} \text{Pwr}_{\text{fc}} \tag{30}$$

where $\bar{H}$ is the actual operation time in a year and its value is set at 8000 h/year; PI_{NG} and PI_{steam} denote the unit costs of natural gas and steam, respectively; PI_{fuel} and PI_{ele} denote the unit prices of heat and electrical power that can be charged to the customers, respectively. Note that the other variables in the above equations have already been defined in the unit models.

In the second term on the right side of eq 24, the annualization factor ϕ can be computed with the well-known formula

$$\phi = \frac{\xi(1+\xi)^Y}{(1+\xi)^Y - 1} \tag{31}$$

where ξ is the annual interest rate (which has been set to be 5% in all case studies) and Y is the expected operation life of the hydrogen network (which has been set to 18 years in all case studies). On the other hand, the total capital cost is the sum of individual investments for the new compressors, PSA units, fuel cells and pipelines, i.e.

$$\text{Total Capital Cost} = C_{\text{comp}} + C_{\text{PSA}} + C_{\text{fc}} + C_{\text{pipe}} \tag{32}$$

The above four capital investments can be estimated according to the following formulas:

$$C_{\text{comp}} = \sum_{\text{com}\in\mathbf{COM}'} e_{\text{com}}(a_{\text{comp}} + b_{\text{comp}}\text{Pwr}_{\text{com}}) \tag{33}$$

$$C_{\text{PSA}} = \sum_{\text{pur}\in\mathbf{PUR}'} e_{\text{pur}}(a_{\text{PSA}} + b_{\text{PSA}}\sum_{i\in\mathbf{I}} F_{i,\text{pur}}) \tag{34}$$

$$C_{\text{fcell}} = a_{\text{fcell}}\sum_{\text{fc}\in\mathbf{FC}'} \text{Pwr}_{\text{fc}} \tag{35}$$

$$C_{\text{pipe}} = \sum_{(i,j)\in\text{PIPE}'} e_{i,j}^{\text{pipe}}\bar{l}_{i,j}(a_{\text{pipe}} + b_{\text{pipe}}d_{i,j}^{\ 2}) \tag{36}$$

The cost coefficients in eqs 33 −36 assume the following constant values: a_{comp} = 178.83 (k$), b_{comp} = 2.97 (k$/kW), a_{PSA} = 666.34 (k$), b_{PSA} = 459.48 (k$/MMscfd), a_{fcell} = 2242.99 ($/kW), a_{pipe} = 4.97 ($/m), and b_{pipe} = 17.76 ($/(m in^2)). Note also that $\bar{l}_{i,j}$ and $d_{i,j}$ in eq 36 denote the length (meters) and diameter (inches), respectively, of pipeline between source i and sink j. The former is treated as a given model parameter in this study, while the latter can be computed as

$$d_{i,j} = \sqrt{\frac{4F_{i,j}\rho^{\circ}}{\pi u\rho}} \tag{37}$$

where u is the superficial velocity whose value is usually fixed between 15 and 30 m/s; ρ and ρ° denote the gas density in connection (i, j) and that under the standard operating conditions, respectively.

4.2. Example 1. A test problem is analyzed here to demonstrate the usefulness of the proposed models. Let us consider the flow diagram presented in Figure 4, which can be viewed as the typical hydrogen network in an existing refinery.

dx.doi.org/10.1021/ie5037726 | Ind. Eng. Chem. Res. 2014, 53, 20204−20222

The steam reforming plant, which consists of the hydrogenation unit (HU), the steam reforming reactors (SMR), and the purifier (PSA1), is encircled with dotted line. It is also assumed in this example that the hydrogenation unit, HU, can be treated as a standard hydrogen user in which excess hydrogen is used for maximizing reaction conversion and that the two product streams are produced with an embedded separator. The 0% stream contains predominately methane for steam reforming, while the 75% product can be regarded as a potential hydrogen source. In addition, the other existing units in this hydrogen network include two hydrogen users (A and B) and four compressors (OM1, OM2, OMNG, and OMHU). Note that the off gases from hydrogen users and the residue stream from the PSA unit are all consumed in the fuel gas system.

The nominal operating conditions at the inlets and outlets of all hydrogen users are shown in Tables 1 and 2, respectively.

Table 1. Nominal Inlet Conditions of Existing Hydrogen Users in Example 1

sink	flow rate (MMscfd)	purity (vol %)	pressure (psi)
A	90.00	92.00	600
B	110.00	92.00	1200
HU	27.63	92.00	400

Table 2. Nominal Outlet Conditions of Existing Hydrogen Users in Example 1

source	flow rate (MMscfd)	purity (vol %)	pressure (psi)
A	40.00	75.00	400
B	20.00	80.00	700
HU	10.00	75.00	300

Note that the listed nominal flow rates and concentrations of units A and B obviously must satisfy the corresponding model constraints; therefore, the parameters $\overline{f}_{sr}^{H_2}$ and $\overline{f}_{sr}^{CH_4}$ (sr = A, B) can be determined by substituting these nominal values into eqs 11 and 12. As mentioned before, $\overline{f}_{sk}^{min}$ and $\overline{y}_{sk}^{min}$ (sk = A, B) in eqs 8 and 9 denote the lower bounds of the inlet hydrogen flow rate and concentration, respectively, and their values are chosen conservatively at the nominal levels in this study. To avoid computational difficulties, the upper concentration limits at sources A and B, i.e., $\overline{y}_A^{max}$ and $\overline{y}_B^{max}$, are set at 76.65 vol % and 81.60 vol %, respectively (which are both slightly higher than the nominal values given in Table 2). Finally, the inlet concentration and the outlet flow rate and concentration of unit HU are fixed at their nominal values according to eq 17 and eqs A.3 and A.4 in the Appendix.

The equipment specifications of all available compressors are given in Table 3. As for the purifier **PSA1**, it is assumed that (1) its maximum capacity is 350.0 MMscfd, (2) its operating pressure is 300 psi, and (3) the discharge pressure of residue stream is 30 psi. The unit costs of raw materials adopted in this study are 4500 $/MMscfd (natural gas) and 10 $/ton (steam), while the selling prices of electricity and fuel are chosen to be 0.1 $/kW-h and 3.0 $/MMBtu, respectively.

Table 3. Operating Conditions of Existing Compressors in Example 1

compressor	P_{com}^{in} (psi)	P_{com}^{out} (psi)	$\overline{f}_{com}^{max}$ (MMscfd)
OM1	300	600	103.50
OM2	300	1200	126.50
OMNG	15	400	79.44
OMHU	300	400	31.77

In this example, it is assumed that the number of each type of new units cannot exceed one, i.e., $N_{comp} = N_{PSA} = N_{fcell} = 1$. The corresponding superstructure can be found in Figure 5. For the sake of brevity, the lengths of all embedded pipelines ($\overline{l}_{i,j}$) are presented in the Supporting Information. As mentioned before, if a new compressor is allowed in the revamp design, then it is necessary to enumerate all possible combinations of its suction and discharge pressures based on the operating pressures at all available sources and sinks. By following the procedure suggested by Chiang and Chang,[19] an exhaustive list can be generated (see Table 4). The same approach can also be applied to produce the pressure combinations in Table 5 for the new PSA unit.

The optimization runs for solving the test problem were carried out in the GAMS 23.7 environment on a PC with Intel Core i7-2600 3.40 GHz processor. Although BARON is generally believed to be a better solver for locating the global optimum of a MINLP model, DICOPT was executed repeatedly with 3000 sets of randomly generated initial guesses. The latter solution strategy is generally more efficient for the present problem because the former may not converge even in a long period of time (e.g., 1 week). To demonstrate the advantages of using the improved models, two different MINLP models were adopted to generate the optimal designs.

(1.) The hydrogen production plant was treated as a single unit in a conventional mathematical programming model. All equations in the Appendix were used, while the consumption rates of raw materials and utilities were also calculated according to eqs 14 and 19−22 just for comparison purposes. The resulting optimal network is presented in Figure 6. Note that the process configuration of the steam reforming plant is the same as that in the original network in Figure 4. In this design, an additional PSA unit is introduced into the downstream network to recover and recycle the hydrogen in the off gases from units A and B. As a result, the consumption rate of natural gas can be lowered to 76.7% of the original level.

(2.) The hydrogenation and steam reforming reactions and the pressure swing adsorption process in the hydrogen plant were incorporated in the superstructure as three separate units. The improved unit models described in sections 3.1 and 3.2 and the conventional models given in sections A.2−A.4 in the Appendix were utilized to construct the MINLP model. The corresponding optimal solution can be summarized with Figure 7. When compared with the conventional network design in Figure 6, it can be observed that adding extra PSA units is no longer necessary in this case. The off gases from units A and B can be processed in the existing unit PSA1 instead, while the residue stream from hydrogenation process, i.e., unit HU, is compressed with a new unit, NM20, to facilitate hydrogen recovery in PSA1. The natural gas is consumed in this improved design at an even lower rate (which is about 73.9% of the original level).

The operating costs, capital costs, and total annual costs of the aforementioned designs are compared in Table 6. It can be clearly observed that (1) the TAC savings of hydrogen integration schemes produced with the conventional and improved models can reach 17.02% and 20.44% of the original level, respectively, and (2) the latter is superior to the former in terms of both operating expenditure and capital investment.

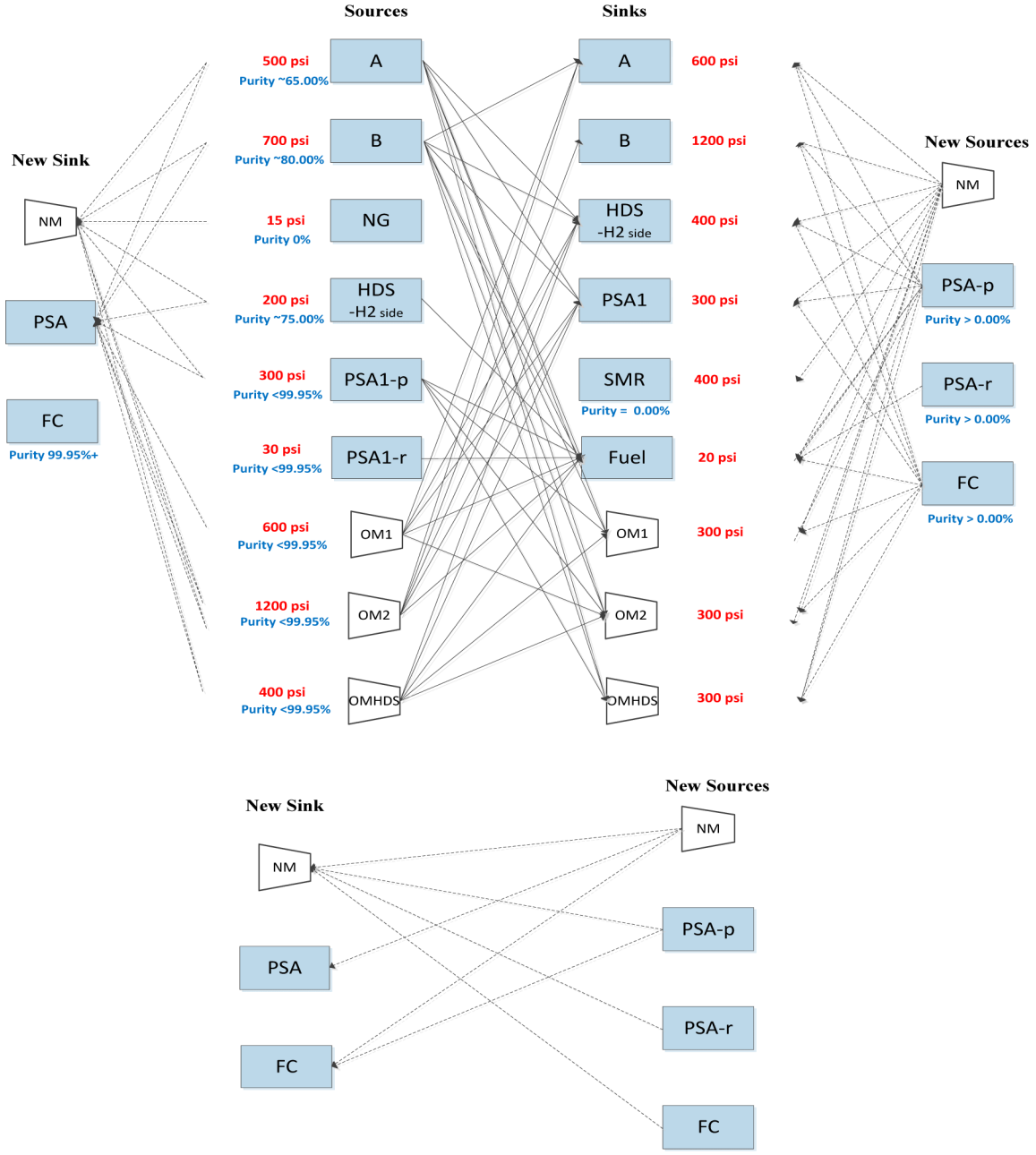

Figure 5. Suprsturcture used in example 1.

5. TWO EFFECTIVE MULTIPERIOD DESIGN STRATEGIES

As indicated in the Introduction, the conventional design considerations are incomprehensive. To address this concern, the aforementioned MINLP model can be reformulated in a straightforward fashion to generate multiperiod designs. It should be noted that these designs were traditionally produced to accommodate the *anticipated* seasonal variations in model parameters, e.g., see Van den Heever and Grossmann.[23] Because the number of variables in the resulting model is several times that in the original version, the corresponding optimization runs may not converge easily. For the purpose of circumventing potential difficulties in numerical computation, another strategy has also been developed in this study to manually synthesize flexible structures based on multiple single-period designs. The detailed descriptions of these two alternative design strategies are presented below.

5.1. Programming Approach. To facilitate clear explanation, an additional label set should be introduced:

$$\mathbf{P} = \{p \mid p \text{ is the label of a distinct operating period during a year}\}$$

Because the unit models in sections 3.1 and 3.2 and those in sections A.2−A.4 in the Appendix are clearly still applicable in each period, it is necessary to introduce only an extra subscript p to every process variable and every model parameter in the corresponding constraints. Consequently, eqs 26−30 can also be adopted for computing the operating costs in period p according to the given operation time ($\bar{H}_p$), the unit costs of natural gas and steam ($PI_{NG,p}$ and $PI_{steam,p}$), and the unit prices

dx.doi.org/10.1021/ie5037726 | Ind. Eng. Chem. Res. 2014, 53, 20204−20222

Table 4. Alternative Operating Pressures of a New Compressor in Example 1

no.	P^{in}_{com} (psi)	P^{out}_{com} (psi)	pressure ratio
1	400	600	1.50
2	400	1200	3.00
3	400	700	1.75
4	700	1200	1.71
5	300	600	2.00
6	300	1200	4.00
7	300	400	1.33
8	300	700	2.33
9	600	1200	2.00
10	600	700	1.17
11	100	600	6.00
12	100	1200	12.0
13	100	400	4.00
14	100	300	3.00
15	100	700	7.00
16	15	400	26.7

Table 5. Alternative Operating Pressures of a New PSA Unit in Example 1

no.	P^{in}_{pur} (psi)	$P^{out,prod}_{pur}$ (psi)	$P^{out,resid}_{pur}$ (psi)
1	700	700	70
2	400	400	40
3	600	600	60
4	500	500	50

of heat and electrical power ($PI_{fuel,p}$ and $PI_{ele,p}$) in this period. By summing the cost contributions in all periods, the total annual operating cost can then be determined on the basis of eq 25.

Although as mentioned above the same formulations can be adopted to model all units in any period, the logic constraints concerning the new units and pipelines must be modified. In the former case, eq 1 should be replaced with the following two constraints:

$$e_{neq,p}B^{L}_{neq} \le \sum_{i\in\mathbf{I}} F_{i,neq,p} \le e_{neq,p}B^{U}_{neq} \tag{38}$$

$$e_{neq,p} \le e_{neq} \tag{39}$$

where $e_{neq,p} \in \{0,1\}$, neq $\in$ **NEQ**, and $p \in$ **P**, while eqs 2−4 are still valid. On the other hand, eq 5 in the latter case should be changed to

$$e^{pipe}_{i,j,p}B^{L}_{i,j} \le F_{i,j,p} \le e^{pipe}_{i,j,p}B^{U}_{i,j} \tag{40}$$

$$e^{pipe}_{i,j,p} \le e^{pipe}_{i,j} \tag{41}$$

where $e^{pipe}_{i,j,p} \in \{0,1\}$ and $(i, j) \in$ **PIPE**′. Thus, instead of using eqs 33−36, the corresponding capital costs should be calculated according to the following formulas:

$$C_{comp} = \sum_{com\in\mathbf{COM}'} e_{com}(a_{com} + b_{com} \max_{p} Pwr_{com,p}) \tag{42}$$

$$C_{PSA} = \sum_{pur\in\mathbf{PUR}'} e_{pur}(a_{PSA} + b_{PSA} \max_{p} \sum_{i\in\mathbf{I}} F_{i,pur,p}) \tag{43}$$

$$C_{fcell} = a_{fcell} \sum_{fc\in\mathbf{FC}'} \max_{p} Pwr_{fc,p} \tag{44}$$

$$C_{pipe} = \sum_{(i,j)\in\mathbf{PIPE}'} e^{pipe}_{i,j}\overline{l}_{i,j}(a_{pipe} + b_{pipe} \max_{p} d^{2}_{i,j,p}) \tag{45}$$

Consequently, eqs 24, 31, and 32 can then be utilized for evaluating the total annual cost associated with a multiperiod design.

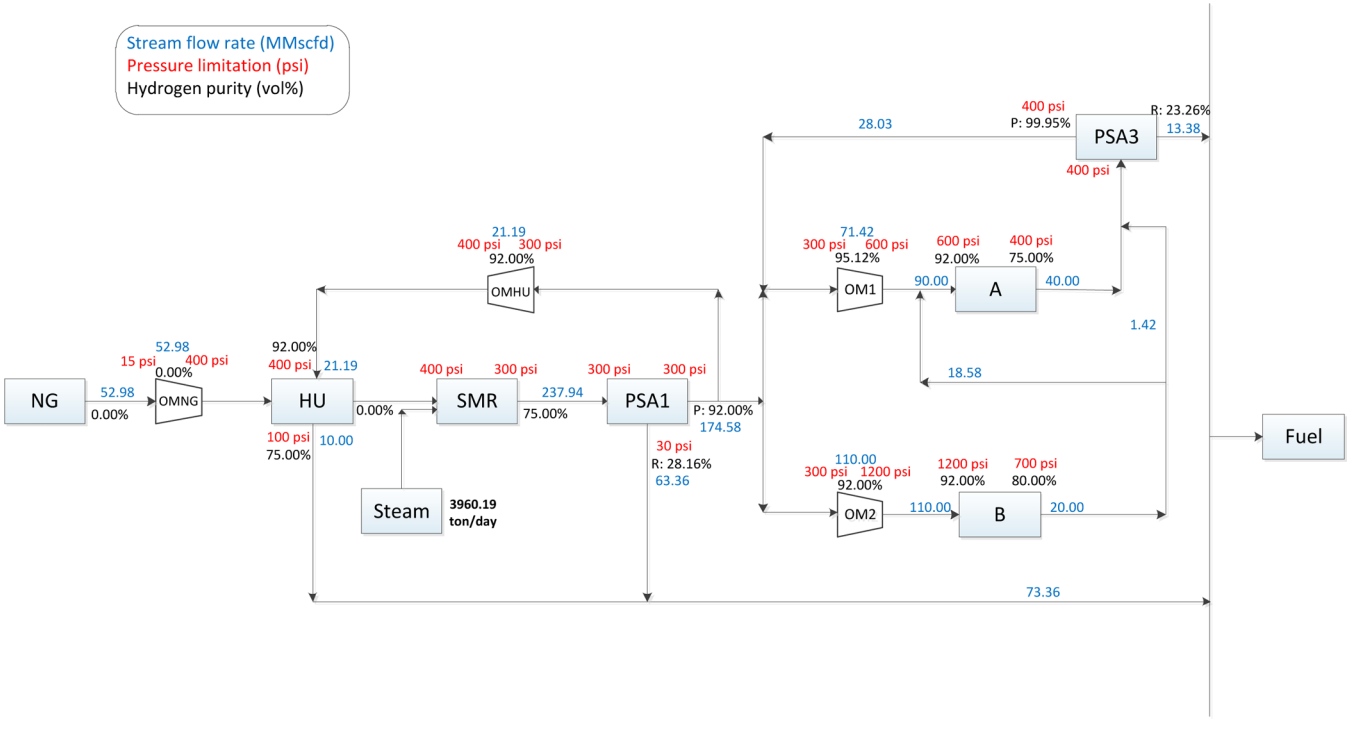

Figure 6. Network design obtained with conventional formulation in example 1.

dx.doi.org/10.1021/ie5037726 | Ind. Eng. Chem. Res. 2014, 53, 20204−20222

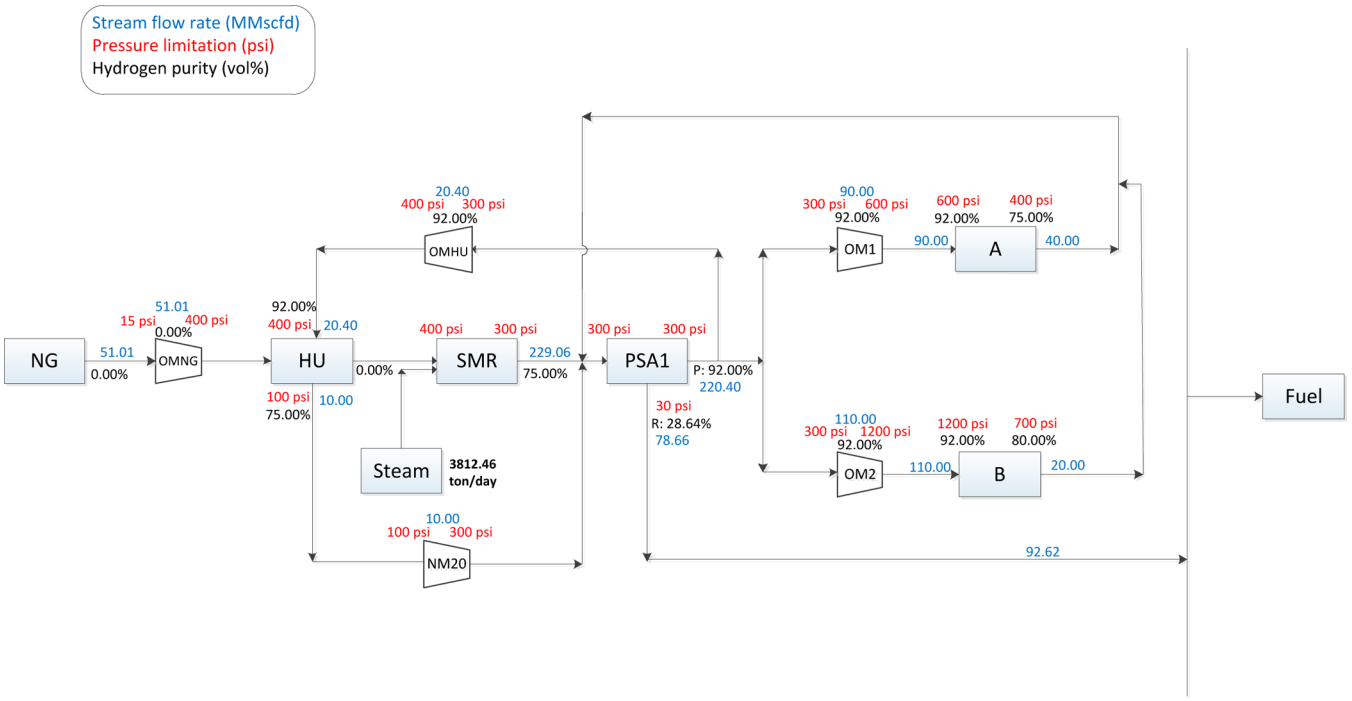

Figure 7. Network design obtained with improved formulation in example 1.

Table 6. Cost Summary of Example 1 (million $/year)

	original design	conventional scheme	improved scheme
natural gas	103.63	79.47	76.51
steam	17.21	13.20	12.70
electricity	17.42	14.26	14.44
fuel	−13.93	−6.04	−5.06
operating cost	124.33	100.90	98.60
compressor	0.00	0.00	1.12
PSA	0.00	19.70	0.00
piping	0.00	3.86	2.15
annualized total capital cost	0.00	2.27	0.31
TAC	124.33	103.17	98.91

5.2. Heuristic Approach. The aforementioned programming approach calls for solving a single mathematical program that minimizes the total annual cost (TAC), which is determined under the implied assumption that the *given durations* of all periods in a year are fixed. Other than the potential computational difficulties encountered in executing the optimization runs, the resulting designs are often suboptimal for actual operations because the given period lengths may have to be adjusted in response to the unexpected external disturbances in raw material supplies and/or customer demands. Thus, an alternative heuristic approach is also taken in the present study to circumvent these drawbacks. In particular, a single-period model is first constructed and solved to produce the optimal design for each period individually. A timesharing strategy is then applied to integrate all such single-period designs so as to reduce the overall capital investment as much as possible while still keeping the operating costs in every period at the desired levels. In addition to their economic benefits, such designs should be considered to be more flexible because they are optimal despite unforeseen changes in the operation schedule.

Jiang and Chang[24] have made use of this idea to develop heuristic rules for generating multiperiod HEN designs based on the heat-transfer areas needed to facilitate the operation of every single-period network. In the present applications, it is assumed that only the PSA units and compressors may be used to handle different streams in different periods. In the former case, because the capital cost of a PSA unit is a function of its capacity only, the heat-transfer areas used in the existing heuristic procedure[24] can be simply replaced with PSA throughputs to produce the corresponding timesharing schemes. On the other hand, it can be observed from eq 33 and eq A.8 in the Appendix that the capital cost of a compressor depends upon its throughput and also the ratio between the discharge and suction pressures. Sorokes[25] further suggested that, other than the power requirement, the operating conditions of a chosen compressor must also satisfy the practical constraints defined by (1) an upper bound on the discharge pressure, (2) a lower bound on the suction pressure, and (3) a maximum throughput limit. On the basis of these considerations, a systematic procedure has been developed to identify the timesharing mechanisms in a multiperiod design.

(1.) Produce an optimal single-period design for each period according to the corresponding model parameters. Create two compressor lists and one stream list on the basis of *all* such designs:

i. All existing compressors are ranked in list A according to their maximum deliverable powers. The largest power provider is given the highest priority.
ii. All new compressors are ranked in list B according to their maximum deliverable powers. The largest power provider is given the highest priority.
iii. All streams with compression needs are ranked in list C according to their power consumption rates. The largest power consumer is given the highest priority.

(2.) Select list A and treat it as the *current* compressor list.
(3.) Select the first candidate in the current compressor list.

dx.doi.org/10.1021/ie5037726 | *Ind. Eng. Chem. Res.* 2014, 53, 20204−20222

(4.) Assign the highest ranked stream in *every* period in list C to the chosen compressor. More specifically, exactly one stream in each period should be assigned and then checked to determine if the following requirements can be satisfied:

i. The upper limit of compressor discharge pressure must be larger than or equal to the target pressure of stream;
ii. The lower limit of compressor suction pressure must be smaller than or equal to the initial pressure of stream;
iii. The maximum allowable compressor throughput must be larger than or equal to the streamflow rate.

If the assigned stream fails to meet one or more constraints, than the next one in the same period in the stream list should be considered. This step should be repeated until a qualified candidate can be found.

(5.) If a suitable stream in every period can be assigned to the chosen compressor, remove the assigned streams from list C and then go to step 6. Otherwise, reconsider the highest ranked stream in the *unassigned* period in list C.

i. If one (or both) pressure constraint is violated, then consider compressing this stream in two (or three) separate stages. One of them should be assigned to the chosen compressor to facilitate the largest achievable pressure change, while the remaining one(s) treated as new stream(s) and placed in list C. All streams in the resulting list should then be ranked again.
ii. If the capacity constraint is violated, then consider processing only a split branch of this stream and its flow rate should be the maximum allowable throughput of the chosen compressor. The other branch should be treated as a new stream and placed in list C. All streams in the resulting list should then be ranked again

(6.) Remove the chosen compressor from the current compressor list.

(7.) Repeat steps 3−6 until all candidates in the current compressor list are exhausted.

(8.) Select list B as the current compressor list. Repeat Steps 3−7 until all candidates in the stream list are exhausted.

5.3. Example 2. Let us revisit the first illustrative example and modify some of the model parameters. For illustration convenience, this revised test problem is termed example 2. To be more specific, it is assumed in the present example that (1) units A and B have to be operated differently in three distinct periods every year according to Tables 7 and 8; (2) the unit costs of natural gas, electricity, and steam vary from one period to another according to Table 9; and (3) all other constants remain unchanged.

Table 7. Nominal Inlet Conditions of Existing Hydrogen Users in Example 2

sink	flow rate in period 1 (MMscfd)	flow rate in period 2 (MMscfd)	flow rate in period 3 (MMscfd)	purity (vol %)	pressure (psi)
A	90.00	94.00	98.00	92.00	600
B	110.00	112.00	117.00	92.00	1200

For comparison purpose, three synthesis strategies can be adopted to generate (1) one single-period design for multiperiod operation, (2) a multiperiod design by integrating several single-period designs via timesharing schemes, and (3) a multiperiod design by solving the multiperiod programming model. These three scenarios are discussed in detail in the following.

Table 8. Nominal Outlet Conditions of Existing Hydrogen Users in Example 2

source	flow rate in period 1 (MMscfd)	flow rate in period 2 (MMscfd)	flow rate in period 3 (MMscfd)	purity (vol %)	pressure (psi)
A	40.00	43.00	45.00	75.00	400
B	20.00	21.00	23.00	80.00	700

Table 9. Unit Costs of Raw Materials and Utilities in Example 2

	period 1	period 2	period 3
natural gas ($/MMscf)	3535	4600	4302
electricity ($/kWh)	0.18	0.07	0.09
steam ($/ton)	8.86	12.51	9.06

5.3.1. Strategy 1. To demonstrate the advantages of multiperiod designs, it is revealing to first produce an "optimal" single-period design and calculate the corresponding TAC(s) under the modified operating conditions and unit utility costs. For this purpose, the following procedure has been followed:

1. Select the operating conditions of a particular period from Table 7 and the corresponding unit costs from Table 8.
2. Solve a single-period programming model to minimize TAC according to the selections made in step 1. Note that the resulting network structure is assumed to be unchanged in all other periods.
3. Fix the network structure (which is determined in step 2), and then solve the single-period programming model repeatedly for all periods not selected in step 1 to minimize their respective total operating costs.
4. The total annual cost can be determined by adding the annualized capital cost (which is obtained in step 2) and the total operating costs in all periods (which can be calculated from the results obtained in steps 2 and 3).

Clearly this calculation procedure is applicable to all three periods in the present example for determining three optimal single-period designs and their TACs. The resulting structure for period 1 can be found in Figure 8, while those for periods 2 and 3 are essentially the same; thus, only the latter is given in Figure 9. It can be observed that, in this example, the unit price of electricity exerts a significant impact on the process configuration. Because the electricity price is exceptionally high in period 1, a very large hydrogen output flow from the steam reforming plant is called for to meet the needs not only in units A and B but also those in the fuel cell. On the other hand, the fuel cells are excluded in the other two periods due to the relatively low electricity costs. The raw material costs in these two cases are reduced mainly by recovering and recycling hydrogen from off gases.

5.3.2. Strategy 2. To facilitate implementation of the proposed heuristic procedure for creating the timesharing scheme (see section 5.2), let us first list the existing and new compressors and streams and their power consumption rates in all aforementioned single-period designs in Tables 10 and 11, respectively. It should be noted that, if these single-period designs are to be operated individually in their intended periods, every new compressor is bound to be idle in at least one period.

dx.doi.org/10.1021/ie5037726 | Ind. Eng. Chem. Res. 2014, 53, 20204−20222

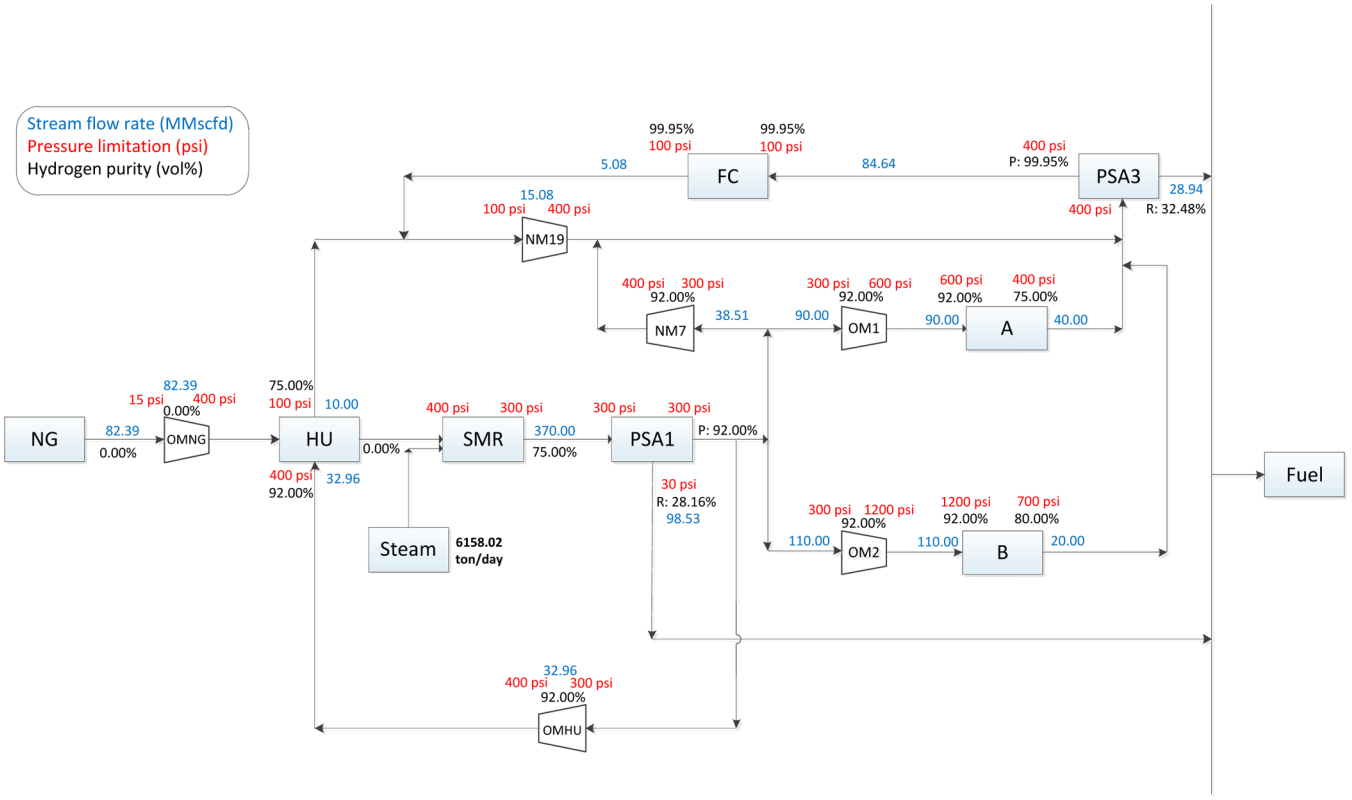

Figure 8. Optimal single-period design for period 1 in example 2.

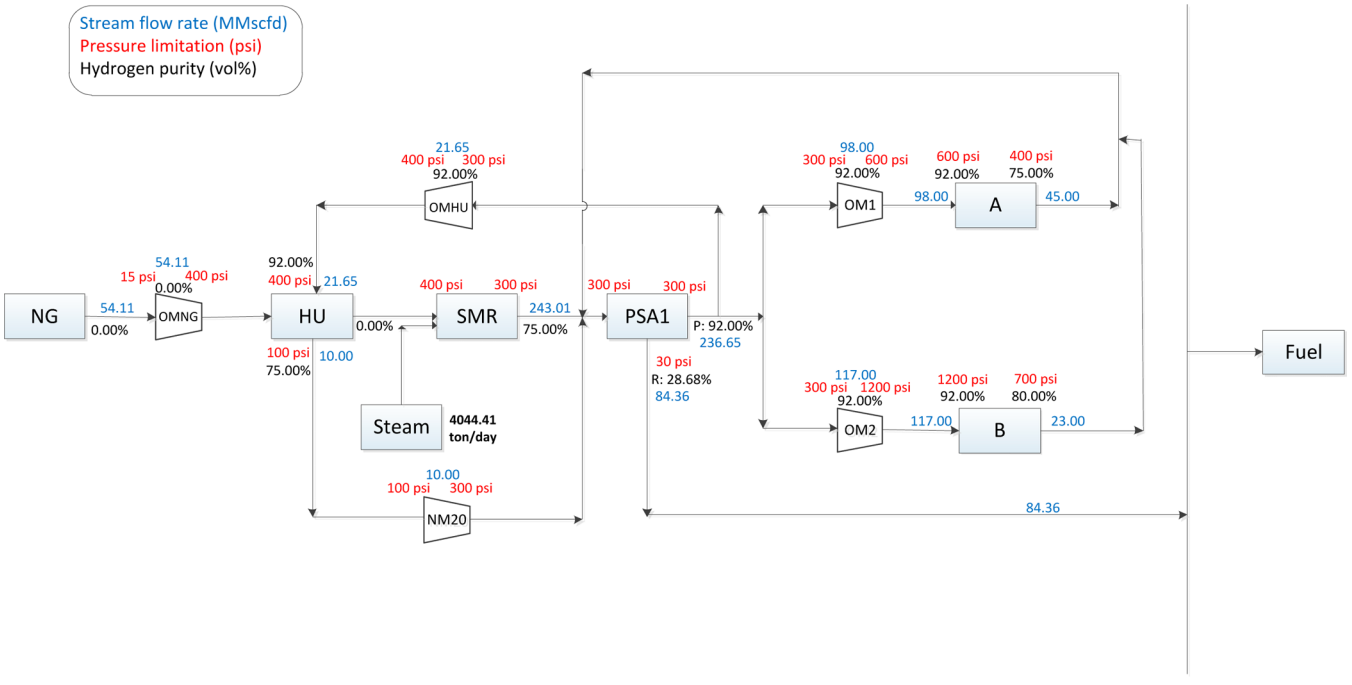

Figure 9. Optimal single-period design for period 3 in example 2.

The existing and new compressors and the compressed streams in different periods can be ranked separately according to the corresponding power consumption rates (see Tables 10 and 11). The resulting list A and list B are presented in Table 12, while list C can be found in Table 13. Note that the additional process data provided in these two tables can be extracted from the optimal single-period designs mentioned above. By following the proposed heuristic procedure, one can manually produce the timesharing scheme in Table 14. Note that only two new compressors, i.e., NM19 and NM7, are put in use in this case. Compressor NM20, which is needed in the single-period designs for periods 2 and 3, is now replaced by NM19, which originally is idle during these two periods.

dx.doi.org/10.1021/ie5037726 | Ind. Eng. Chem. Res. 2014, 53, 20204−20222

Table 10. Power Consumption Rates of Existing Compressors and Streams in the Single-Period Designs

	power (MW)		
	period 1	period 2	period 3
stream 1 (OM1)	1.71	1.78	1.86
stream 2 (OM2)	4.63	4.72	4.93
stream 3 (OMHU)	0.24	0.15	0.16

Table 11. Power Consumption Rates of New Compressors and Streams in the Single-Period Designs

	power (MW)		
	period 1	period 2	period 3
stream 4 (NM7)	0.285	0.00	0.00
stream 5 (NM19)	0.63	0.00	0.00
stream 6 (NM20)	0.00	0.315	0.315

Table 12. Ordered Lists of Existing and New Compressors in Example 2

compressor label	power (MW)	maximum capacity (MMscfd)	suction pressure (psi)	discharge pressure (psi)
OM2	4.93	117.00	300	1200
OM1	1.86	98.00	300	600
OMHU	0.24	35.00	300	400
NM19	0.63	15.07	100	400
NM20	0.315	10.00	100	300
NM7	0.285	38.51	300	400

Table 13. Ordered Stream List in Example 2

stream label	period	power (MW)	initial/target pressures (psi)	flow rate (MMscfd)
stream 2	3	4.93	300/1200	117.00
stream 2	2	4.72	300/1200	112.00
stream 2	1	4.63	300/1200	110.00
stream 1	3	1.86	300/600	98.00
stream 1	2	1.78	300/600	94.00
stream 1	1	1.71	300/600	90.00
stream 5	1	0.63	100/400	15.08
stream 6	2	0.315	100/400	10.00
stream 6	3	0.315	100/400	10.00
stream 4	1	0.285	300/400	38.51
stream 3	1	0.24	300/400	32.96
stream 3	3	0.16	300/400	21.65
stream 3	2	0.15	300/400	20.82

5.3.3. Strategy 3. As described in section 5.1, a multiperiod programming model can also be formulated and solved for optimal hydrogen integration in the present example. The resulting designs in the first two periods are shown in Figures 10 and 11, respectively, while the third is omitted because its structure is the same as that in period 1. Note that the structural features of these networks are in general very similar to those of their single-period counterparts. However, these traits are less obvious because a compromise among the different contributions from all periods may have to be achieved to minimize the total annual cost.

The operating costs, capital costs, and total annual costs of all aforementioned designs are compared in Table 15, and a brief cost analysis is given below.

Table 14. Timesharing Scheme Identified in Example 2

stream no.	period	OM2 4.93 (MW)	OM1 1.86 (MW)	OMHU 0.24 (MW)	NM19 0.63 (MW)	NM7 0.285 (MW)
stream 2	1	×				
stream 1	1		×			
stream 3	1			×		
stream 5	1				×	
stream 4	1					×
stream 2	2	×				
stream 1	2		×			
stream 3	2			×		
stream 6	2				×	
stream 2	3	×				
stream 1	3		×			
stream 3	3			×		
stream 6	3				×	

(1.) It can be observed that by incorporating the proposed model modifications, the TAC of any single-period design (evaluated with strategy 1) is significantly lower than that of the original network. However, any such design should be optimal only in one period of a year but may not be suitable for the other time intervals. For example, one can clearly see from Figures 8 and 9 and Table 11 that the two new compressors adopted in the first single-period design are not exactly compatible with the needs in the next two periods.

(2.) If strategy 2 is adopted to synthesize a multiperiod design, all optimal single-period structures can be incorporated in the resulting network. When compared with the scenarios evaluated with strategy 1, this unique feature facilitates a significant cut in the total operating cost and therefore further reduction in the total annual cost (see Table 15). Note that these financial benefits are realized in part by lowering the increase in total capital cost with the timesharing mechanisms.

(3.) Because the optimal trade-off between operating and capital costs can be achieved in the multiperiod design created with strategy 3, the TAC in this case is the lowest among all options. However, the corresponding optimization run usually requires a very long computation time which is, on average, 10 times greater than that needed to produce a single-period design.

6. ADDITIONAL CASE STUDIES

Let us next consider a conventional hydrogen network studied in Hallale and Liu.[8] Figure 12 shows an adapted version of this network, which consists of

- six hydrogen using units, i.e., the hydrocracker (HC), the cracked naphtha hydrotreater (CNHT), the diesel hydrotreater (DHT), the jet fuel hydrotreater (JHT), the naphtha hydrotreater (NHT), and the isomerization plant (IS4);
- two hydrogen production units, i.e., the steam reforming plant and the continuous catalytic reformer (CCR); and
- four compressors (OM1, OM2, OMNG, and OMHU).

Notice that only the steam reforming plant in Figure 12 is not the same as that in the original configuration. Specifically, three component units, i.e., the hydrogenation unit (HU), reforming unit (SMR), and pressure swing adsorption unit (PSA1), are now introduced to replace the single hydrogen production unit considered in the conventional modeling approach. It is assumed that all hydrogen-using units in this

dx.doi.org/10.1021/ie5037726 | Ind. Eng. Chem. Res. 2014, 53, 20204−20222

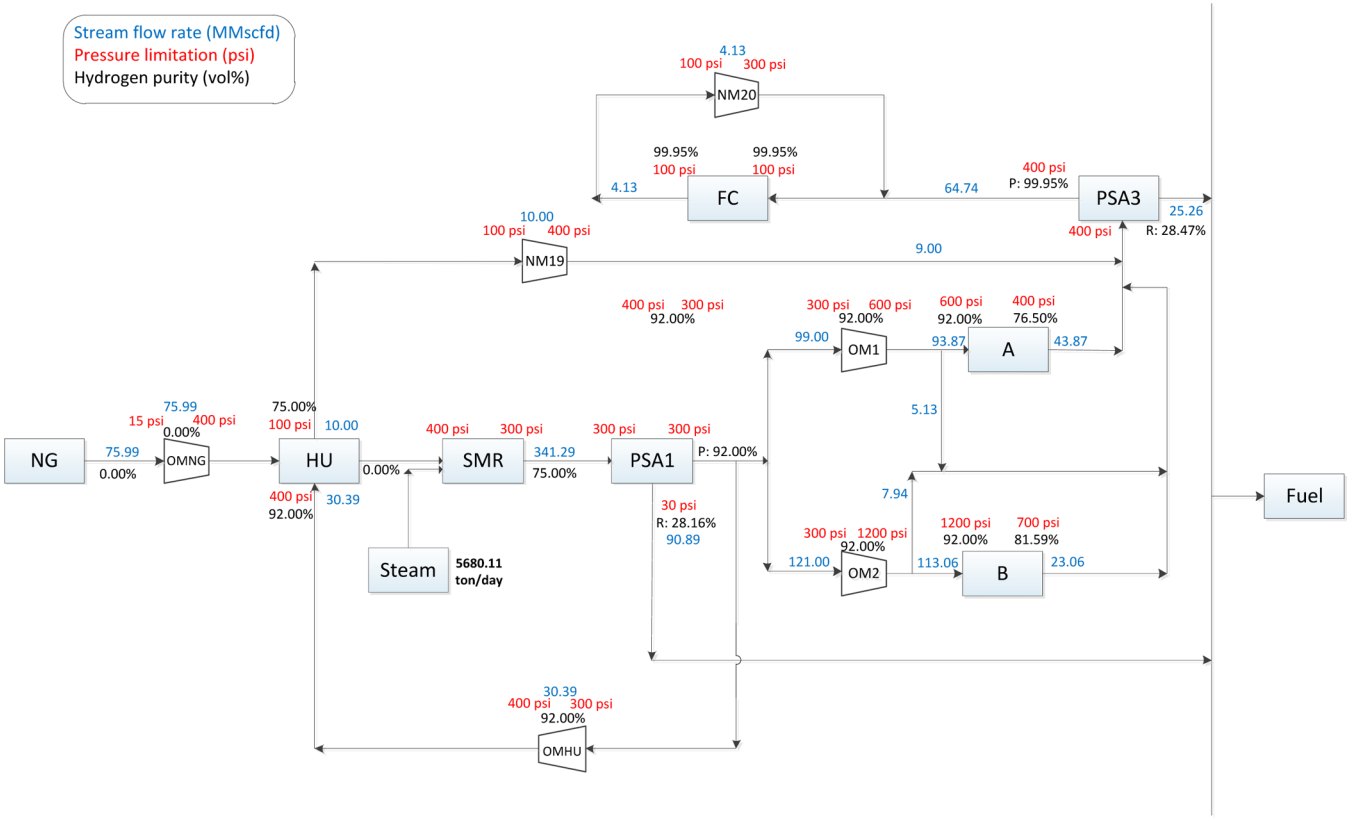

Figure 10. Optimal multiperiod design for period 1 in example 2.

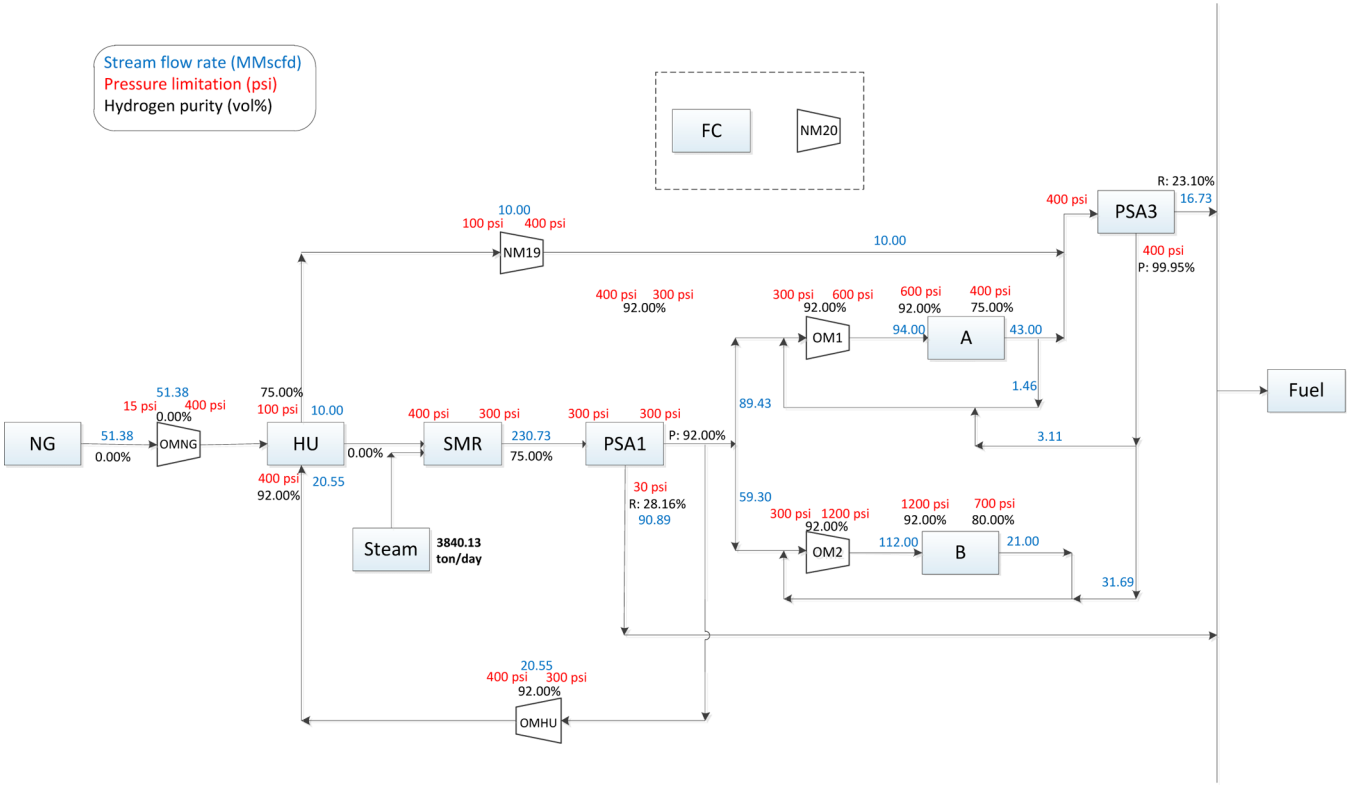

Figure 11. Optimal multiperiod design for period 2 in example 2.

system have to be operated according to Tables 16 and 17, and the unit costs of natural gas, electricity, and steam in three different periods are listed in Table 18. As for the purifier PSA1, it is assumed that (1) its maximum capacity is 50.0 MMscfd, (2) its operating pressure is 300 psi, and (3) the discharge pressure of residue stream is 30 psi.

dx.doi.org/10.1021/ie5037726 | Ind. Eng. Chem. Res. 2014, 53, 20204−20222

Table 15. Cost Summary of Example 2 (Million $/Year)

	original network	strategy 1 (period-1 structure)	strategy 1 (period-3 structure)	strategy 2	strategy 3
operating cost (period 1)	35.59	5.09	30.12	5.09	9.77
operating cost (period 2)	38.24	33.93	31.35	31.35	0.31.12
operating cost (period 3)	38.60	30.56	31.78	31.78	30.59
total operating cost	112.42	69.58	93.25	68.22	71.49
compressor	0.00	3.08	1.11	3.08	1.98
PSA	0.00	52.86	0.00	52.86	42.02
fuel cell	0.00	215.13	0.00	215.13	175.04
piping	0.00	5.40	1.26	6.66	4.73
annualized total capital cost	0.00	23.64	0.20	23.75	19.13
TAC	112.42	93.21	93.45	91.97	90.62

To facilitate concise illustration, the design problem considered here is termed example 3. Note that the three synthesis strategies adopted in example 2 have also been used to generate network designs in the present example, and the resulting cost summary is given in Table 19. For the sake of brevity, the detailed synthesis results are placed in the Supporting Information. By comparing Tables 15 and 19, one can see that the trends observed in both cases are very similar; therefore, all conclusions of the cost analysis in example 2 are also applicable here.

Table 16. Nominal Inlet Conditions of Existing Hydrogen Users in Example 3

sink	flow rate in period 1 (MMscfd)	flow rate in period 2 (MMscfd)	flow rate in period 3 (MMscfd)	purity (vol %)	pressure (psi)
HC	38.78	39.11	26.64	92.00	2000
DHT	11.31	10.26	9.85	75.97	600
CNHT	8.21	8.35	5.12	86.53	500
JHT	8.65	6.79	5.11	75.00	500
NHT	12.08	12.12	5.47	71.44	300

Table 17. Nominal Outlet Conditions of Existing Hydrogen Users in Example 3

source	flow rate in period 1 (MMscfd)	flow rate in period 2 (MMscfd)	flow rate in period3 (MMscfd)	purity (vol %)	pressure (psi)
HC	11.29	11.75	7.637	75.00	1200
DHT	8.61	8.91	7.16	70.00	400
CNHT	3.47	3.49	1.96	75.00	350
JHT	4.32	4.05	1.01	65.00	350
NHT	6.55	6.57	2.31	60.00	200

Table 18. Unit Costs of Raw Materials and Utilities in Example 3

	period 1	period 2	period 3
natural gas ($/MMscf)	3535.0	4600.0	4302.0
electricity ($/kWh)	0.18	0.07	0.125
steam ($/ton)	8.86	12.51	9.06

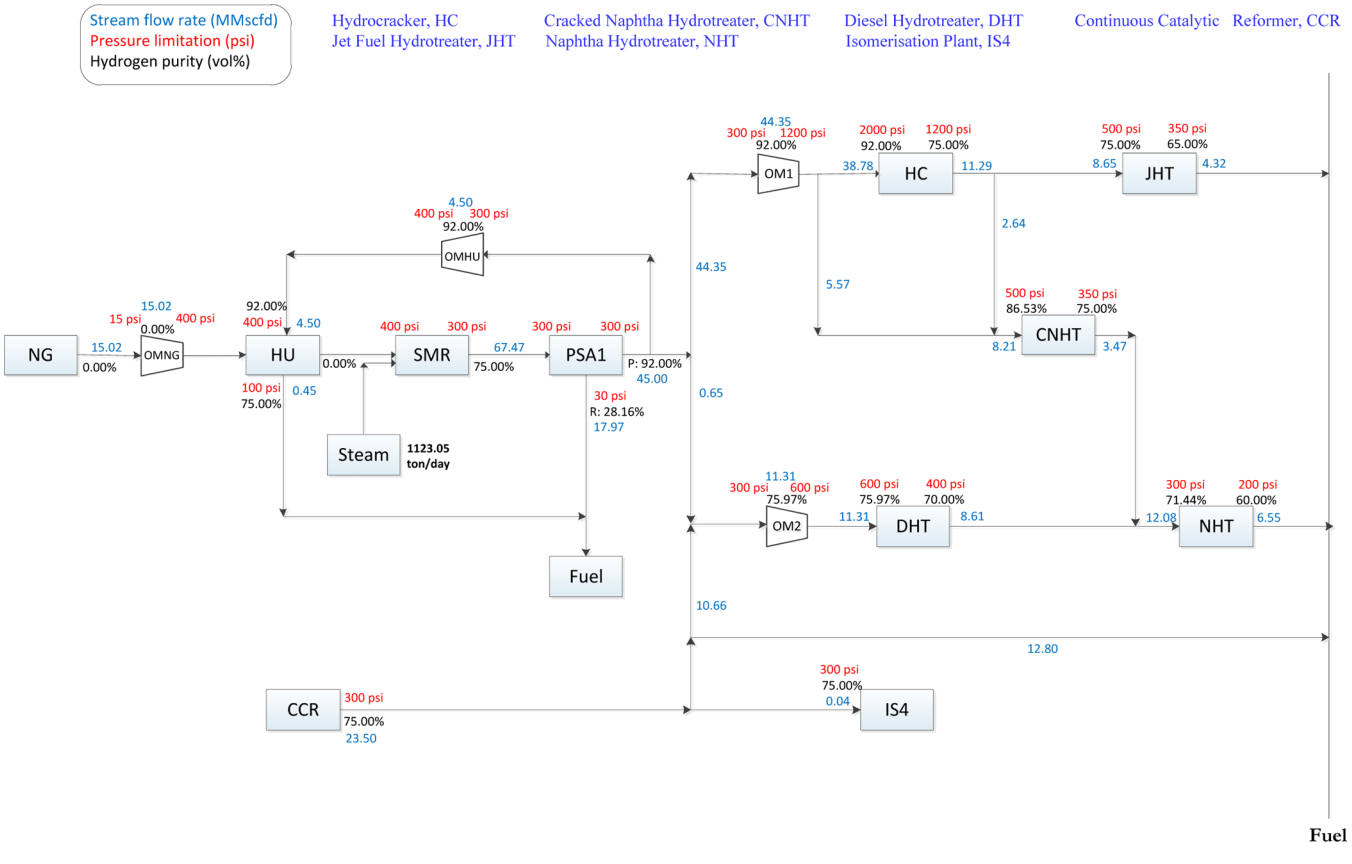

Figure 12. Original hydrogen network in example 3.

dx.doi.org/10.1021/ie5037726 | Ind. Eng. Chem. Res. 2014, 53, 20204−20222

Table 19. Cost Summary of Example 3 (Million $/Year)

	original network	strategy 1 (period-1 structure)	strategy 1 (period-2 structure)	strategy 1 (period-3 structure)	strategy 2	strategy 3
operating cost (period 1)	7.92	1.32	5.95	2.34	1.32	1.39
operating cost (period 2)	7.68	5.23	5.08	6.48	5.08	5.06
operating cost (period 3)	5.27	2.32	2.92	0.33	0.33	1.14
total operating cost	20.87	8.87	13.95	9.15	6.73	7.59
compressor	0.00	0.93	0.79	0.70	1.36	1.10
PSA	0.00	14.21	0.00	14.24	14.24	14.21
fuel cell	0.00	39.33	0.00	55.59	55.59	39.33
piping	0.00	1.99	1.08	1.72	3.10	2.22
annualized total capital cost	0.00	4.83	0.16	6.18	6.38	4.86
TAC	20.87	13.70	14.11	15.33	13.08	12.45

Although strategy 3 yields a cost-optimal design according to Table 19, the corresponding TAC is at minimum only under the assumption that the *given durations* of all periods in a year are fixed. Because these time intervals must be adjusted in response to the unexpected changes in raw material supplies and/or customer demands, this assumption cannot be held in most actual operations. On the other hand, because all optimal single-period structures are realizable in the network generated with strategy 2, the corresponding design is clearly more flexible. Therefore, for any realistic application, both strategies can be considered because their pros and cons have to be evaluated on a case-by-case basis.

7. CONCLUSIONS

The conventional programming approach to generate hydrogen networks has been modified in this work to circumvent drawbacks concerning (1) unreasonable unit models of the hydrogen users and producers and (2) incomprehensive design considerations. The former modifications usually facilitate identification of better design options. To address the latter issue, the seasonal variations in model parameters and the options to add extra auxiliary units have also been incorporated in a multiperiod formulation in the present study. As an alternative to this brute-force numerical optimization method, a systematic timesharing algorithm is also devised to manually integrate the conventional single-period designs to form a less economical but more flexible network structure for operations in all periods. Finally, three examples are presented in this paper to demonstrate the feasibility and effectiveness of the proposed design methods.

APPENDIX: CONVENTIONAL UNIT MODELS

The following unit models are essentially the same as those adopted in Chiang and Chang.[19] Note that all notations in these models are also explained in Nomenclature to facilitate illustration clarity.

A.1. Hydrogen-Using Units

$$\sum_{i\in\mathbf{I}} F_{i,\mathrm{sk}} = \overline{f}_{\mathrm{sk}} \tag{A.1}$$

$$\sum_{i\in\mathbf{I}} F_{i,\mathrm{sk}} y_i = \overline{f}_{\mathrm{sk}}\,\overline{y}_{\mathrm{sk}} \tag{A.2}$$

$$\sum_{j\in\mathbf{J}} F_{\mathrm{sr},j} = \overline{f}_{\mathrm{sr}} \tag{A.3}$$

$$y_{\mathrm{sr}} = \overline{y}_{\mathrm{sr}} \tag{A.4}$$

where sk ∈ **SK** and **SK** denotes the set of all inlets of hydrogen users; sr ∈ **SR** and **SR** denotes the set of all outlets of hydrogen users; $F_{i,\mathrm{sk}}$ denotes the flow rate of a stream from source i to sink sk (MMscfd); $F_{\mathrm{sr},j}$ denotes flow rate of a stream from source sr to sink j (MMscfd); $\overline{f}_{\mathrm{sk}}$ and $\overline{f}_{\mathrm{sr}}$ are model parameters which represent the flow rates (MMscfd) at sink sk and source sr, respectively; $\overline{y}_{sk}$ and $\overline{y}_{sr}$ are model parameters which denote the hydrogen concentrations (vol %) at the sink sk and source sr, respectively.

A.2. Compressors

$$\sum_{j\in\mathbf{J}} F_{\mathrm{com},j} = \sum_{i\in\mathbf{I}} F_{i,\mathrm{com}} \tag{A.5}$$

$$y_{\mathrm{com}} \sum_{j\in\mathbf{J}} F_{\mathrm{com},j} = \sum_{i\in\mathbf{I}} F_{i,\mathrm{com}} y_i \tag{A.6}$$

$$\sum_{i\in\mathbf{I}} F_{i,\mathrm{com}} \le \overline{f}_{\mathrm{com}}^{\max} \tag{A.7}$$

$$\eta_{\mathrm{com}}\mathrm{Pwr}_{\mathrm{com}} = \left(\left(\frac{P_{\mathrm{com}}^{\mathrm{out}}}{P_{\mathrm{com}}^{\mathrm{in}}}\right)^{\gamma_{\mathrm{com}}-1/\gamma_{\mathrm{com}}} - 1\right) TC_{p,\mathrm{com}}\rho_{\mathrm{com}}^{\mathrm{o}} \sum_{i\in\mathbf{I}} F_{i,\mathrm{com}} \tag{A.8}$$

$$\rho_{\mathrm{com}}^{\mathrm{o}} = \frac{\rho_{\mathrm{H_2}}^{\mathrm{o}}}{M_{\mathrm{H_2}}} y_{\mathrm{com}} + \frac{\rho_{\mathrm{CH_4}}^{\mathrm{o}}}{M_{\mathrm{CH_4}}}(1 - y_{\mathrm{com}}) \tag{A.9}$$

$$C_{p,com}\rho_{\mathrm{com}}^{\mathrm{o}} = C_{p,\mathrm{H_2}}\frac{\rho_{\mathrm{H_2}}^{\mathrm{o}}}{M_{\mathrm{H_2}}} y_{\mathrm{com}} + C_{p,\mathrm{CH_4}}\frac{\rho_{\mathrm{CH_4}}^{\mathrm{o}}}{M_{\mathrm{CH_4}}}(1 - y_{\mathrm{com}}) \tag{A.10}$$

$$\gamma_{\mathrm{com}} = 1 + \left(\frac{y_{\mathrm{com}}}{\gamma_{\mathrm{H_2}} - 1} + \frac{1 - y_{\mathrm{com}}}{\gamma_{\mathrm{CH_4}} - 1}\right)^{-1} \tag{A.11}$$

where com ∈ **COM** and **COM** represents the set of compressors; $F_{i,\mathrm{com}}$ denotes the flow rate of a stream from source i to compressor com (MMscfd); $\overline{f}_{\mathrm{com}}^{\max}$ is a model parameter that represents the maximum allowable throughput (MMscfd) of compressor com; y_{com} denotes the hydrogen concentration (vol %) at the exit of compressor com; $\mathrm{Pwr}_{\mathrm{com}}$ is the power (MW) required for operating compressor com; $C_{p,\mathrm{com}}$ is the heat capacity (kJ/(mol K)) of the stream entering compressor com; γ_{com} is the heat capacity ratio of the stream entering compressor com; $\rho_{\mathrm{com}}^{\mathrm{o}}$ is the molar density (mol/scf) of the stream entering compressor com under standard conditions; $P_{\mathrm{com}}^{\mathrm{in}}$ and $P_{\mathrm{com}}^{\mathrm{out}}$ denote the suction and discharge

dx.doi.org/10.1021/ie5037726 | Ind. Eng. Chem. Res. 2014, 53, 20204−20222

pressures (psi) of compressor com, respectively; T is the compressor inlet temperature (which is set to be constant at 298.15 K); η_{com} is compressor efficiency (which is fixed at 0.8 in this study). In this compressor model, the thermodynamic properties of hydrogen and methane are assumed to be constants, i.e., C_{p,H_2} = 0.0288 (kJ/(mol K)), γ_{H_2} = 1.42, C_{p,CH_4} = 0.0357 (kJ/(mol K)), and γ_{CH_4} = 1.30.

A.3. Pressure Swing Adsorption Units

$$y_{pur}^{in} \sum_{i\in \mathbf{I}} F_{i,pur} = \sum_{i\in \mathbf{I}} F_{i,pur} y_i \tag{A.12}$$

$$y_{pur}^{prod} \sum_{j\in \mathbf{J}} F_{pur,j}^{prod} = R \sum_{i\in \mathbf{I}} F_{i,pur} y_i \tag{A.13}$$

$$\sum_{i\in \mathbf{I}} F_{i,pur} = \sum_{j\in \mathbf{J}} F_{pur,j}^{prod} + \sum_{j\in \mathbf{J}} F_{pur,j}^{resid} \tag{A.14}$$

$$\sum_{i\in \mathbf{I}} F_{i,pur} y_i = y_{pur}^{prod} \sum_{j\in \mathbf{J}} F_{pur,j}^{prod} + y_{pur}^{resid} \sum_{j\in \mathbf{J}} F_{pur,j}^{resid} \tag{A.15}$$

$$\sum_{i\in \mathbf{I}} F_{i,pur} y_i \le \overline{fy}_{pur}^{max} \tag{A.16}$$

$$y_{pur}^{in} \ge \overline{y}_{pur}^{in} \tag{A.17}$$

$$y_{pur}^{prod} \ge \overline{y}_{pur}^{out} \tag{A.18}$$

where pur ∈ **PUR** and **PUR** denotes the set of all available PSA units; $F_{i,pur}$ denotes the flow rate of a stream from source i to unit pur (MMscfd); $F_{pur,j}^{prod}$ denotes the flow rate of product stream from unit pur to sink j (MMscfd); $F_{pur,j}^{resid}$ denotes the flow rate of residue stream from unit pur to sink j (MMscfd); $\overline{fy}_{in,pur}^{max}$ is the maximum allowable processing rate of hydrogen in unit pur, whose value is set to be 200 MMscfd in this study; y_{pur}^{in} denotes the hydrogen concentration (vol %) at the inlet of unit pur; $\overline{y}_{pur}^{in}$ (= 80.0 vol %) is a model parameter which represents the lower bound of hydrogen concentrations at the inlet of unit pur; y_{pur}^{resid} and y_{pur}^{prod} denote the volumetric concentrations (vol %) of hydrogen in the product and residue streams, respectively, of PSA unit pur; $\overline{y}_{pur}^{out}$ (= 99.95 vol %) is the lower bound of y_{pur}^{prod}; R (= 0.9) is a dimensionless constant representing the hydrogen recovery ratio.

A.4. Fuel Cells

$$y_{fc}^{in} \sum_{i\in \mathbf{I}} F_{i,fc} = \sum_{i\in \mathbf{I}} F_{i,fc} y_i \tag{A.19}$$

$$\mathrm{Pwr}_{fc} = \eta_{fc} \mathrm{LHV}_{H_2} \frac{\rho_{H_2}^{o}}{M_{H_2}} \sum_{i\in \mathbf{I}} F_{i,fc} y_i \tag{A.20}$$

$$(1-\mu_{fc}) \sum_{i\in \mathbf{I}} F_{i,fc} y_i = y_{fc}^{out} \sum_{j\in \mathbf{J}} F_{fc,j} \tag{A.21}$$

$$\eta_{fc} = \frac{\mu_{fc} v_c}{1.25} \tag{A.22}$$

$$\sum_{i\in \mathbf{I}} F_{i,fc} y_i \le \overline{fy}_{fc}^{max} \tag{A.23}$$

$$y_{fc}^{in} \ge \overline{y}_{fc}^{min} \tag{A.24}$$

$$y_{fc}^{out} = \overline{y}_{fc}^{out} \tag{A.25}$$

where fc ∈ **FC** and **FC** represents the set of fuel cells; $F_{i,fc}$ denotes the flow rate of a stream in superstructure from source i to unit fc (MMscfd); $F_{fc,j}$ denotes the flow rate of a stream in superstructure from unit fc to sink j (MMscfd); $\overline{fy}_{fc}^{max}$ is the maximum allowable hydrogen feed rate of fuel cell fc, whose value is set to be 180 MMscfd in this study; y_{fc}^{in} denotes the hydrogen concentration (vol %) at the inlet of fuel cell fc; $\overline{y}_{fc}^{min}$ (= 99.95 vol %) and $\overline{y}_{fc}^{out}$ (= 99.95 vol %) are both model parameters which denote the lower bound of hydrogen concentration at the inlet and the fixed hydrogen concentration at the outlet of fuel cell fc, respectively; Pwr_{fc} is the power generated by fuel cell fc (MW); η_{fc} is the electrical conversion efficiency of fuel cell fc, and its value should be between 0.55 and 0.60; μ_{fc} denotes the fuel utilization rate of fuel cell fc, and its value should be between 0.86 and 0.94; v_c is the operating voltage of fuel cell and a value of 0.8 (volt) has been chosen in the present study; $\overline{\rho}_{H_2}^{o}$ is the density of hydrogen under standard conditions, i.e., 0.003 lb/scf; M_{H_2} denotes the molecular weight of hydrogen, i.e., 2.02 g/mol; LHV_{H_2} is the lower heating value of hydrogen, and its value 229.25 BTU/mol.

A.5. Fuel Gas System

$$Q_{fuel} = \Delta H_{c,H_2}^{o} \frac{\rho_{H_2}^{o}}{M_{H_2}} \sum_{i\in \mathbf{I}} F_{i,fuel} y_i + \Delta H_{c,CH_4}^{o} \frac{\rho_{CH_4}^{o}}{M_{CH_4}} \sum_{i\in \mathbf{I}} F_{i,fuel} (1-y_i) \tag{A.26}$$

where Q_{fuel} denotes the total heat generation rate of the fuel gas system (MMBTU/day); $F_{i,fuel}$ denotes the flow rate of a stream in superstructure from source i to the fuel gas system (MMscfd); $\overline{\rho}_{CH4}^{o}$ is the density of methane under standard conditions, i.e., 0.024 lbm/scf; M_{CH_4} denotes the molecular weight of methane, i.e., 16.04 g/mol; $\Delta H_{c,H_2}^{o}$ (= 229.25 BTU/mol) and $\Delta H_{c,CH_4}^{o}$ (= 760.88 BTU/mol) denote the heats of combustion of hydrogen and methane, respectively.

■ ASSOCIATED CONTENT

Supporting Information

Lengths of all embedded pipelines and detailed synthesis results. This material is available free of charge via the Internet at http://pubs.acs.org.

■ AUTHOR INFORMATION

Corresponding Author

*Tel: 886-6-2757575, ext. 62663. E-mail: ctchang@mail.ncku.edu.tw.

Notes

The authors declare no competing financial interest.

■ NOMENCLATURE

Sets

I = hydrogen sources
J = hydrogen sinks
PIPE = connection between source and sink in the superstructure
PIPE$_o$ = connection between source and sink in the existing hydrogen network
SR(⊂**I**) = sources associated with hydrogen users
SK(⊂**J**) = sinks associated with hydrogen users

dx.doi.org/10.1021/ie5037726 | Ind. Eng. Chem. Res. 2014, 53, 20204−20222

COM = compressors
COM′(⊂**COM**) = new compressors
PUR = purifiers
PUR′(⊂**PUR**) = new purifiers
FC = fuel cells
FC′(⊂**FC**) = new fuel cells
NEQ = new units
P = periods

Variables

C = capital cost (USD)
$Cost$ = operating cost (USD)
d = pipeline diameter (in)
e = binary variable denoting if an equipment is present in the hydrogen network
F = flow rate of a connection (MMscfd)
f = throughput of a unit (MMscfd)
Pwr = electric power (MW)
Q = fuel value (MMBtu/day)
Rvn = revenue (USD)
TAC = total annual cost (USD)
y = purity (vol %)
Z = hydrogen production rate (MMscfd)

Parameters

a = capital cost coefficient
B = bound
b = capital cost coefficient
C_p = heat capacity at constant pressure (kJ/mol K)
$\overline{f}$ = constant flow rate of hydrogen-containing stream (MMscfd)
$\overline{fy}$ = constant hydrogen flow rate in hydrogen-containing stream (MMscfd)
$\overline{H}$ = annual operating hours (h)
$\overline{l}$ = constant pipeline length (m)
LHV = low heating value of combustion (Btu/mol)
M = molecular weight
N = numbers of new equipment
k, k', k'', k''' = proportionality coefficients
P = pressure (psi)
R = hydrogen recovery ratio
$\overline{r}$ = proportionality constant
T = temperature (K)
u = superficial velocity (m/s)
PI = price per unit quantity
Y = number of years
$\overline{y}$ = constant hydrogen purity (vol %)
ΔH_c^o = heat of combustion (Btu/mol)
ϕ = annualization factor
ξ = fractional interest rate
γ = ratio of heat capacity at constant pressure to that at constant volume
η = efficiency
μ = fuel utilization

Subscripts

com = compressor com ∈ **COM**
ele = electricity
fc = fuel cell fc ∈ **FC**
fuel = fuel system
H2P = hydrogen plant
HU = hydrogenation unit
i = source i ∈ **I**
j = sink j ∈ **J**
NG = natural gas
neq = new equipment neq ∈ **NEQ**
OM-fc = operating and maintenance of fuel cell
p = period p ∈ **P**
pur = pressure swing adsorption pur ∈ **PUR**
SMR = steam reformer
sr = source associated with a hydrogen user sr ∈ **SR**
sk = sink associated with a hydrogen user sk ∈ **SK**

Superscripts

in = inlet
L = lower bound
max = maximum
min = minimum
out = outlet
prod = product
resid = residue
U = upper bound

REFERENCES

(1) Towler, G. P.; Mann, R.; Serriere, A. J.-L.; Gabaude, C. M. D. Refinery hydrogen management: Cost analysis of chemically-integrated facilities. *Ind. Eng. Chem. Res.* **1996**, *35*, 2378−2388.
(2) Alves, J. J.; Towler, G. P. Analysis of refinery hydrogen distribution systems. *Ind. Eng. Chem. Res.* **2002**, *41*, 5759−5769.
(3) El-Halwagi, M. M.; Gabriel, E.; Harell, D. Rigorous graphical targeting for resource conservation via material recycle/reuse networks. *Ind. Eng. Chem. Res.* **2003**, *42*, 4319−4328.
(4) Zhao, Z.; Liu, G.; Feng, X. The integration of the hydrogen distribution system with multiple impurities. *Chem. Eng. Res. Des.* **2007**, *85*, 1295−1304.
(5) Ding, Y.; Feng, X.; Chu, K. H. Optimization of hydrogen distribution systems with pressure constraints. *J. Cleaner Prod.* **2011**, *19*, 204−211.
(6) Zhang, Q.; Feng, X.; Liu, G. L.; Chu, K. H. A novel graphical method for the integration of hydrogen distribution systems with purification reuse. *Chem. Eng. Sci.* **2011**, *66*, 797−809.
(7) Zhang, Q.; Feng, X.; Chu, K. H. Evolutionary graphical approach for simultaneous targeting and design of resource conservation networks with multiple contaminants. *Ind. Eng. Chem. Res.* **2013**, *52*, 1309−1321.
(8) Hallale, N.; Liu, F. Refinery hydrogen management for clean fuels production. *Adv. Environ. Res.* **2001**, *6*, 81−98.
(9) Van den Heever, S. A.; Grossmann, I. E. A strategy for the integration of production planning and reactive scheduling in the optimization of a hydrogen supply network. *Comput. Chem. Eng.* **2003**, *27*, 1813−1839.
(10) Liu, F.; Zhang, N. Strategy of purifier selection and integration in hydrogen networks. *Chem. Eng. Res. Des.* **2004**, *82*, 1315−1330.
(11) Khajehpour, M.; Farhadi, F.; Pishvaie, M. R. Reduced superstructure solution of MINLP problem in refinery hydrogen management. *Int. J. Hydrogen Energy* **2009**, *34*, 9233−9238.
(12) Liao, Z. W.; Wang, J. D.; Yang, Y. R.; Rong, G. Integrating purifiers in refinery hydrogen networks: A retrofit case study. *J. Cleaner Prod.* **2010**, *18*, 233−241.
(13) Kumar, A.; Gautami, G.; Khanam, S. Hydrogen distribution in the refinery using mathematical modeling. *Energy* **2010**, *35*, 3763−3772.
(14) Jia, N.; Zhang, N. Multi-component optimization for refinery hydrogen networks. *Energy* **2011**, *36*, 4663−4670.
(15) Zhou, L.; Liao, Z. W.; Wang, J. D.; Jiang, B. B.; Yang, Y. R. Hydrogen sulfide removal process embedded optimization of hydrogen network. *Int. J. Hydrogen Energy* **2012**, *37*, 18163−18174.
(16) Jiao, Y.; Su, H.; Hou, W. Improved optimization methods for refinery hydrogen network and their applications. *Control Eng. Pract.* **2012**, *20*, 1075−1093.
(17) Wu, S.; Liu, G.; Yu, Z.; Feng, X.; Liu, Y.; Deng, C. Optimization of hydrogen networks with constraints on hydrogen concentration and

pure hydrogen load considered. *Chem. Eng. Res. Des.* **2012**, *90*, 1208−1220.
(18) Wu, S.; Yu, Z.; Feng, X.; Liu, G.; Deng, C.; Chu, K. H. Optimization of refinery hydrogen distribution systems considering the number of compressors. *Energy* **2013**, *62*, 185−195.
(19) Chiang, Y. C.; Chang, C. T. Single-objective and multiobjective designs for hydrogen networks with fuel cells. *Ind. Eng. Chem. Res.* **2014**, *53*, 6006−6020.
(20) Ahmad, M. I.; Zhang, N.; Jobson, M. Modelling and optimization for design of hydrogen networks for multi-period operation. *J. Cleaner Prod.* **2010**, *18*, 889−899.
(21) Spath, P. L., and Mann, M. K. *Life Cycle Assessment of Hydrogen Production via Natural Gas Steam Reforming*; Technical Report NREL/TP-570-27637; National Renewable Energy Laboratory: Golden, CO, 2001.
(22) Posada, A.; Manousiouthakis, V. Heat and power integration of methane reforming based hydrogen production. *Ind. Eng. Chem. Res.* **2005**, *44*, 9113−9119.
(23) Van den Heever, S. A.; Grossmann, I. E. Disjunctive multiperiod optimization methods for design and planning of chemical process systems. *Comput. Chem. Eng.* **1999**, *23*, 1075−1095.
(24) Jiang, D.; Chang, C. T. A new approach to generate flexible multiperiod heat exchanger network designs with timesharing mechanisms. *Ind. Eng. Chem. Res.* **2013**, *52*, 3794−3804.
(25) Sorokes, J. M. Selecting a centrifugal compressor. *Chem. Eng. Prog.* **2013**, *6*, 44−51.